

Comparison of the seismic performance of existing RC buildings designed to different codes

Christos A. Zeris^{*1} and Constantinos C. Repapis^{2a}

¹Department of Civil Engineering, National Technical University of Athens, University Campus, Zografou 15780, Greece

²Department of Civil Engineering, University of West Attica, 250 Thivon and Petrou Ralli Str., Egaleo 12244, Greece

(Received November 7, 2017, Revised March 5, 2018, Accepted April 2, 2018)

Abstract. Static pushover analyses of typical existing reinforced concrete frames, designed according to the previous generations of design codes in Greece, have established these structures' inelastic characteristics, namely overstrength, global ductility capacity and available behaviour factor q , under planar response. These were compared with the corresponding demands at the collapse limit state target performance point. The building stock considered accounted for the typical variability, among different generations of constructed buildings in Greece, in the form, the seismic design code in effect and the material characteristics. These static pushover analyses are extended, in the present study, in the time history domain. Consequently, the static analysis predictions are compared with Incremental Dynamic Analysis results herein, using a large number of spectrum compatible recorded base excitations of recent destructive earthquakes in Greece and abroad, following, for comparison, similar conventional limiting failure criteria as before. It is shown that the buildings constructed in the 70s exhibit the least desirable behaviour, followed by the buildings constructed in the 60s. As the seismic codes evolved, there is a notable improvement for buildings of the 80s, when the seismic code introduced end member confinement and the requirement for a joint capacity criterion. Finally, buildings of the 90s, designed to modern codes exhibit an exceptionally good performance, as expected by the compliance of this code to currently enforced seismic provisions worldwide.

Keywords: existing RC buildings; seismic design code; comparative analysis; nonlinear dynamic analysis; performance evaluation; ductility; behaviour factor

1. Introduction and statement of the problem

Post war recovery following World War II, together with the considerable need for urbanization of the population, brought forward a sharp increase in apartment housing and office space construction in the devastated cities of Southern Europe, in the seismically affected territories around the Mediterranean. The need for new construction, resulted in the gradual replacement of the two to three storey masonry buildings in the post war cities and their expanding suburbs, with medium height reinforced concrete (RC) structures, which were designed and built from the start of the reconstruction period in the early 50's, all the way up to the late 90's, when currently accepted construction standards have been enforced in the execution of RC structures (IAEE 2008). Buildings constructed however, during this period, which form a large portion of today's existing building inventory, were engineered with lower grade material characteristics and below standard design and construction procedures, compared to the currently accepted standards.

Extensive laboratory, analytical and post-earthquake field reconnaissance studies are reported, aimed to evaluate

the seismic performance of such existing RC structures, in scope herein; based on such methods and experience, rapid visual screening empirical methodologies (Thermou and Pantazopoulou 2011, Eleftheriadou and Karabinis 2012) or simplified analysis methods (Borzi *et al.* 2013) have also been proposed, in order to develop large scale vulnerability studies of entire urban complexes either for earthquake preparedness planning or for post-earthquake response scenarios. Vulnerability studies of existing structures have been extended to probabilistic studies and evaluation of performance level exceedance probabilities, for given building types and hazard formulations. These on-going research works attempt to quantify the seismic vulnerability of these structures and, with the advancement of Performance Based Design (PBD) techniques, to establish intervention and rehabilitation programs for these structures to conform to current seismic standards and to develop preparedness or insurance plans. Studies aiming at quantifying the performance characteristics of existing building typologies differ in scope and objectives, either focusing on typical building case studies or attempting to establish building taxonomies and thereby investigating entire groups.

Bracci *et al.* (1995) developed several inelastic complexity models of a 1/8 scale three storey RC building, designed for gravity only, which had been tested on the shake table. Their analyses gave good correlations with the observed damage and proved that the vulnerability of an existing RC building can be predicted by both static and

*Corresponding author, Associate Professor
E-mail: zeris@central.ntua.gr

^aAssistant Professor
E-mail: crepapis@puas.gr

dynamic methods, provided that the inelastic characteristics are adequately modelled and different limiting criteria for establishing damage are used. Nguyen and Nguyen (2016) tested a 1/3 scale model of a typical nonconforming three storey RC building on the shake table and verified analytically the recorded response and seismic performance, using refined finite element analysis. Ghobarah *et al.* (1998) investigated a typical low rise RC building constructed in the United States during the 60s (*vis-à-vis* with a modern design), assessing its seismic performance using both static and dynamic analyses, and accounting for statistical variation in its concrete properties; their analysis gave estimates of the failure probabilities for the case studied, for a 50 year timespan. Hueste and Bai (2007) studied a typical RC flat slab five storey building, deemed to represent typical office building construction in the central United States during the 80s, under static inelastic lateral loads or representative synthetic base excitations. They then proposed three retrofit techniques, in order to upgrade the building response following FEMA 356 recommendations (FEMA 2000). Benavent-Climent and Zahran (2010) investigated by way of inelastic time history analyses, the energy absorption and its storey-wise distribution, of typical RC frames, designed for gravity only, with wide beams on columns. They concluded that these structures tend to form soft storeys and are unable to dissipate as efficiently as ordinary frames the input seismic energy. De Stefano *et al.* (2013), evaluated the response of a four storey RC building designed for vertical loads only, investigating the influence of concrete variability within the structure, using both static pushover (SPO) and dynamic analyses methods. La Brusco *et al.* (2015), Tanganelli *et al.* (2017) also evaluated the response of an existing three storey hospital RC building in Italy, designed by earlier Italian regulations, under different ground motion excitations, modelling assumptions and material characteristics, in order to establish the sensitivity of the seismic performance prediction to these evaluation process uncertainties (Pianigiani and Mariani 2017). Ni (2014) used SPO procedures to assess the seismic performance and retrofit strategies of an existing low rise structure in China. Lima *et al.* (2014) evaluated the modelling uncertainty of several low rise RC structures designed for gravity only, using both SPO and nonlinear time history analyses, in order to evaluate common modelling assumptions.

Along the same lines, several studies have attempted to identify structural classifications of the existing RC building stock for the assessment of their seismic vulnerability, either classified among the typical existing structural systems within a large urban centre in proximity to an active fault (Bala *et al.* 2008) or at the entire national level, whereby entire resistance classes are established based on design code generation (Iervolino *et al.* 2007, Eleftheriadou and Karabinis 2012, Mehani *et al.* 2013). Lynch *et al.* (2011) examined the impact of synthetic ground motions on 20 RC frame buildings in Southern California using nonlinear dynamic analyses and showed that older nonductile RC frame structures have a significant probability of collapsing under a strong earthquake event, while modern construction may be vulnerable due to

rupture directivity and basin effects. Favvata *et al.* (2013) studied existing masonry infilled RC buildings with a soft first storey irregularity.

Repapis *et al.* (2006a, b) investigated the seismic performance of a large set of plane frame configurations of typical existing RC building configurations, built from the 60s through the 90s in Greece and Southern Europe, using SPO procedures. The aim of this work was to establish the inelastic lateral load versus roof deformation characteristics of these structural groups, designed and configured with codes, materials and structural systems appropriate of their time, thereby establishing key response parameters such as the available behaviour factor and global ductility under currently enforced spectral demands.

Zeris *et al.* (2006, 2007) have analysed using different model formulations the typical 60s frame used in their study (denoted herein as K60A59), in order to evaluate the sensitivity of the modelling assumptions (namely, finite element formulation, critical section modelling and modelling of the frame joints) in the seismic performance prediction using static and dynamic inelastic analyses procedures. It was demonstrated that the use of lumped plasticity formulations gave comparable damage prediction in terms of storey drift versus column plastic rotations, compared to spread damage flexibility formulations using fibre section modelling, while conventional deformation interpolation models were overall inaccurate. Further allowance for flexible joints in the flexibility models gave similar plastic rotation variations with storey drift at the critical soft storey columns, however, the location of the soft storey was one floor above.

1.1 Research significance

Given the possible shortcomings of using SPO only for seismic performance predictions (Krawinkler and Seneviratna 1998, Mwafy and Elnashai 2001), the reliability of previously published SPO results by Repapis *et al.* (2006b) is investigated herein through a comparison of the induced damage mechanism and relevant damage quantification indices, with dynamic response predictions under increasing amplitude seismic excitations. The results of this analytical investigation are aimed to provide knowledge of: i) the expected structural behaviour of typical existing RC residential buildings designed to different codes in Greece, classified according to their design period, which is particularly useful for retrofit and strengthening scenarios; and ii) to demonstrate the reliability of standardized assessment procedures using SPO methods, for such buildings, using realistic time history response predictions.

1.2 Scope

Nonlinear incremental dynamic analyses (IDA) are performed on selected typical bare frame RC buildings from Repapis *et al.* (2006b), which are representative of the four generations of existing RC frames in Greece, constructed since the early sixties, following the evolution of seismic design codes. Such an IDA approach was proposed for the

indirect evaluation of the behaviour factor of buildings in the Background Document of EC8 (2004). However, the method was extended in application to seismic hazard analysis, directly relating earthquake magnitude and interstorey drift, the damage index, by Vamvatsikos and Cornell (2003). In the present IDA study, both local and global damage indices are established.

2. Existing RC buildings inventory

2.1 Existing building classification groups

With reference to the entire building whose seismic performance was analysed using SPO procedures in Repapis *et al.* (2006b), in the present study the influence of the construction period (namely the building code / material / construction type generation) is investigated, using the IDA approach. All buildings considered herein are regular in height, of RC construction and they are modelled in planar only excitation; torsional and three-dimensional effects in the response are not covered in this study. Following the evolution of Greek Aseismic Design Codes since their first publication in 1959 (Table 1), the existing RC building systems were classified in terms of geometrical dimensions, material grade, design code generation and construction technique into the following four groups, with the basic differences among the four groups summarized below.

- *Group 60*: Buildings built in the 60s
- *Group 70*: Buildings built in the 70s
- *Group 80*: Buildings built in the 80s
- *Group 90*: Buildings built in the 90s up to date

2.1.1 Evolution of code requirements and relevant detailing practices

Buildings in *Group 60* and *Group 70* were designed in accordance with the requirements of the first Greek Seismic Design Code which was established in 1959 (RD59 1959). The code was the first aseismic design code in Greece and was based on the working stress design methodology. As such, the code stipulated analysis methods and base shear coefficients for lateral inertia loads for seismic load combinations at working stress levels, extending the requirements of allowable stress design under vertical loads, in compliance with DIN 1045 (1972), also in effect. Structural elements of the buildings in this generation were characterized by widely spaced transverse reinforcement and, therefore, very little confinement and no capacity design provisions were used in their design, following contemporary code requirements. Nevertheless, a special check was carried out for the perimeter frame columns and beams, while interior beams were usually designed for gravity loads only. Overall, non seismic nominal dead and live loads were similar to the values specified in Eurocode 1 (EC1 2002). For the seismic load combinations, allowable stresses were increased 20%. The design seismicity was based on a three-zone classification system, with base shear coefficients equal to 4%, 6% and 8% of the vertical loads (dead plus live) for rock and hard soils.

Following a series of devastating earthquakes in Greece in 1978 and 1981, *Group 80* buildings were designed following the Interim Modifications of RD59 (MOD84 1984). Also at working stress level, this aseismic code addendum introduced major modifications (albeit not at the base shear coefficient, for major urban centres in Greece), such as: i) a complete frame analysis methodology rather than the simplified methods used before, ii) triangular inertia load distribution, iii) close stirrup spacing in member critical regions (at 125 mm), continuous within the beam column joint and shear wall edge members with confinement and iv) a weak beam - strong column joint check and a shear resistance check, for which moments based on allowable stress values were used (Anagnostopoulos and Lekidis 1986).

Subsequently, and following a period of parallel application in 1990-1995, *Group 90* structures were designed and detailed following the Greek Code for Design of Concrete Works (EKOS 1991) and the Greek Earthquake Resistant Design Code (NEAK 1995), or (within the last decade), Eurocode 2 (EC2 2002) and Eurocode 8 (EC8 2004). This group of codes were based on the use of partial load factors for load and resistance and design evaluation at the serviceability (vertical load combinations) and the ultimate limit states (vertical and seismic load combinations). Seismic design, among other requirements, enforces more stringent critical region detailing compared to *Group 80* (100 mm maximum stirrup spacing, also continuous within the beam column joint), while, for frame structures, a rational weak beam strong column joint capacity and a shear capacity design are enforced using ultimate flexural resistances.

2.1.2 Analysis procedures

Frame analysis of *Group 60* was based primarily on simplified design models, with the interior frame members being designed for gravity loads only while perimeter frame members being analysed as plane frames under combined lateral and vertical loads. Special care was given to the, corner columns, which were also checked for in plan torsional effects.

2.1.3 Geometry and form

Buildings of *Group 60* were typically four to six storeys high and regular in plan, with column spacing between 3.0 to 4.0 m bay widths. *Group 60* columns sections were relatively narrow, reflecting the tendency for economy in concrete usage since it was in situ mixed and manually conveyed and placed, as well as because of the relatively low level of seismic actions. No shear walls were used in this building group; however, common to this group and, in fact, the entire construction in Greece was the use of nonstructural clay brick infills (not in the scope of the present investigation). Compared to today's construction standards, *Group 60* frames had relatively short bay widths; this relatively dense column spacing of the 60s was increased to between 5.0 and 6.0 m bay widths for *Group 70*, while the number of floors increased in this generation to seven or eight. Overall, this structural form remained unchanged in *Groups 80* and *90*, with wider bay sizes being

used in these cases, up to 7.0 m bay width. One common characteristic from *Group 80* onwards, increasing in trend, was the use of RC shear walls, consisting primarily of an isolated elevator / stair well core and (later) distributed perimeter shear walls. Their width ranged from 15 cm in the 70s, 20 cm in the 80s and 25 cm in the 90s. A minimum of 30cm panel width is currently enforced (EC8 2004).

2.1.4 Construction materials

Construction materials for *Group 60* were: DIN 1045 B160 concrete (site mixed), with a mean cube strength of 160 Kp/cm², or grade C12 per EC2 (2004) and smooth steel reinforcement grade DIN StI (grade S220). With the introduction of ready mix concrete in the 70s, *Group 70* materials were B225 concrete, or grade C16 (EC2 2004) and deformed steel grade DIN StIII (grade S400). The majority of the *Group 90* buildings were built with minimum C25 concrete (EC2 2004) and deformed steel grade S500.

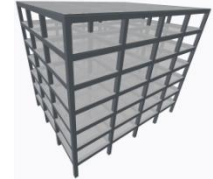
2.2 Building geometry and design details

All buildings considered herein were regular in height and bay width. Based on the typical building geometry above, building K60A59 (*Group 60*) was five storeys high, with a storey height of 3.00 m and a constant bay width of 3.50 m in each direction (K60A59, see Fig. 1). Buildings K70A59 (*Group 70*) and K80A84 (*Group 80*) were seven storeys high, also with a 3.00 m tall storey height throughout; the bay width, in this case, was chosen to be 6.00 m in each direction. All building forms were four by three bays in plan, as shown in Fig. 1 and Table 1.

Furthermore, all buildings were bare frames, despite the fact shear walls were typically included in the lateral resisting system, from *Group 80* onwards, either as a central core at the elevator shaft and/or distributed walls in the perimeter. Therefore, building K80A84 was also designed without the core shear wall in order to compare with the earlier bare frame constructions of K60A59 and K70A59, respectively. In order to assess the vulnerability of a larger proportion of existing regular RC buildings, concentrated mostly in seismicity zones I and II, two frames in *Group 60* were considered, namely K60A59 and K60A59-II. These were assumed to be located in the low and intermediate seismicity zones I and II, respectively, and were accordingly



**K60A59, K60A59-II,
K60AEC8**



K70A59, K80A84

Fig. 1 Selected building forms according to building form notation

designed. Furthermore, an additional frame, denoted K60AEC8 was considered, which had the geometry and occupancy loads of K60A59 and was designed in accordance with the design and detailing requirements of EC8 (2004), as the conforming frame benchmark case. In this case, it was assumed that the structure was located in the same seismicity area as K60A59, also belonging to seismic zone I (of a three zone system), nowadays characterized by an effective peak ground acceleration (*PGa*) of 0.16 g (EC8 2004).

Despite the difference in design code evolution, the building designs for residential and office uses have remained practically constant up to today, since their specification in the 1945 Greek Loadings Code (LC45 1945). Based on this code specified nominal loads, the design load included the self-weight, a distributed in plan surcharge of 2.50 kN/m² for flooring and light moveable internal partitions and a live load of 2.00 kN/m², for residential occupancy. Furthermore, a double wythe 25 cm thick perimeter infill wall load of 3.60 kN/m was included along all the perimeter beams.

Both buildings K60A59, five storeys high, had a storey height of 3.00 m, a regular bay width of 3.50 m and uniform slab thickness of 12 cm. The member dimensions of K60A59 were as follows: columns 35 cm square at the first (ground) floor, 30cm square at the second floor and 25 cm square from the third floor up. Because of the influence of the higher seismic zone, column size and reinforcement ratio were slightly increased for K60A59-II: in this case, columns 35 cm square were used in the first two floors, 30 cm square at the third floor and 25 cm square from the fourth floor up. All the beams and for both buildings were 20 cm by 50 cm, with light reinforcement, due to the dense

Table 1 Building Code generations and related frame typology and characteristics

Year	Regulation	Design Type	Material properties		Form (and Building Designation)
1960	1959 Royal Decree	Allowable Stress	B160 (C12)	StI (S220) smooth	3.5m span, Simplified Analysis, Full or partial infills, no wall. (K60A59, K60A59-II for seismicity zones I and II, resp.)
1970			B225 (C16)	StIII (S400) ribbed	5.0 m-7.0 m, Wall core, infills and Pilotis, Frame Analysis (K70A59)
1985	MOD84				Triangular seismic distr., Critical region details, Partial capacity design (weak beam, $M_{R,all}$). (K80A84)
1995	NEKOS (CEB90)NEAK	SLS/ULS	C16	S400 ribbed	Triangular / spectral seismic distribution, Critical zone detailing, confinement, Capacity design (weak beam + shear, M_{Rd})
2000	EKOS 2000 EAK 2000		C20	S500 ribbed	Rational changes for harmonization with EN 1998
2010	Also EN 1992 - 1998		C25	B500c ribbed	EN 1992 - EN 1998 (K60AEC8)

column spacing and relatively light live loads specified.

These are compared in terms of design requirements evolution to the conforming benchmark building K60AEC8, which was morphologically similar to K60A59 and conformed to the currently enforced seismic standards (EC8 2004), had column dimensions which were 40 cm square in the three lower storeys which subsequently, reduced to 35 cm square to the fourth storey and 30 cm in the last storey. Beams in this case were also 20 cm by 50 cm.

Buildings K70A59 and K80A84 seven storeys high, had a storey height of 3.00 m, a regular bay width of 6.0 m and uniform slab thickness of 16 cm. Column dimensions were: 60 cm square (interior) and 90/25 cm² rectangular (exterior), at the first two storeys, being subsequently reduced by 10 cm (interior) and 20 cm (exterior) for every two storeys, respectively, up to the seventh storey, where the columns were 30 cm square (interior) and 35/25 cm² rectangular (exterior). Similarly, the dimensions of the beams were 20/60 cm² along the interior frames and 25/50 cm² along the perimeter frames. The cross-sections and the reinforcement detailing are presented in Appendix A.

3. Description of the inelastic building models

All the frames were modelled as plane frames with rigid diaphragmatic action at each floor, using the Drain-2DX software (Prakash *et al.* 1993), for the nonlinear static and time history analysis of frames. For modelling the members, a two component lumped plasticity line element, with bilinear hardening flexural characteristics at the hinges. In order to calculate the relevant hinge characteristics as well as the maximum flexural rotation capacity of the RC members, the ultimate curvature was established using fibre section analysis (see also the evaluation of the hinge Limit Criteria in Section 4). However, the case of possible inadequate splice of the column reinforcement at the base was ignored.

Beams were modelled as T-section beams, while the columns were prismatic and the building joints assumed to be infinitely stiff. For the hinge mechanical characteristics the actual reinforcement passing through the critical region was considered: for the beams, common to standard practice at the time, top steel typically included half plus one of the bent up bars from the two neighbouring midspan sections plus any top additional steel and including the reinforcement within the slab effective width. Along the same lines, the bottom steel at the ends included the remaining unbent midsection bars, accounting, in the case of buildings belonging to *Group 60*, for area reduction to include improper anchorage of the bottom steel at the joint. For the columns the axial load-bending moment interaction diagrams were specified, again using the entire section reinforcement configuration active in the response direction of interest.

In accordance with current assessment procedures for existing structures, the nonlinear flexural characteristics of all the member end critical region sections were established using average material properties. For buildings K60A59 and K60A59-II, an unconfined concrete compressive strength equal to 16 MPa was used, with this value

becoming equal to 22.5 MPa for the buildings K70A59 and K80A84. Any modifications in the concrete stress-strain diagram due to confinement (particularly K80A84) were evaluated following the confined concrete model in EC2 (2004), also adopted in EKOS (1991). Similarly, for the two K60A59 buildings, the average yield and ultimate stresses of the reinforcement were set equal to 310 MPa and 420 MPa, respectively, with these values becoming equal to 430 MPa and 630 MPa, for the buildings K70A59 and K80A84.

The loading of the buildings along with the seismic excitation was assumed to be equal to the dead loads, as described, with ψ_2 , the combination coefficient per EC2 (2004) for the acting live load, equal to 30%. Following the program conventions, inertia masses were directly obtained from the loads and were lumped at the beam-column joints.

4. Seismic performance evaluation

The seismic performance of existing RC frames has been studied for a wider range of both regular and irregular (as well as infilled) existing RC structures in all *Groups 60* to *90*, using SPO methods; the estimation of the building's inelastic characteristics accounted, in addition to design, analysis and morphology particularities above, for adjustments in the ultimate limit state design characteristics, the target point estimation and a variety of possible limiting performance criteria, encountered in such buildings (Repapis *et al.* 2006a). The comparative results among different building generations, irregularity forms and perimeter infill wall configurations have been reported in Repapis *et al.* (2006b). The outcome of these SPO studies, for each building, included the structural overstrength, the available global ductility capacity and behaviour factor, the mechanism and limiting criterion (LC) that characterized failure, for particular SPO lateral load profiles and the vulnerability of these structures, under current design target spectral deformations, obtained from equivalent single degree of freedom target point estimations.

In the present study, the seismic performance (inelastic characteristics, damage indices quantification, failure form and mechanism identification, local force and deformation demands and so on) from SPO are compared herein with corresponding results using actual dynamic response, under recorded base excitation, following incremental dynamic analysis procedures (IDA, Vamvatsikos and Cornell 2003). For meaningful comparisons, all base excitations are suitably scaled to the design response spectral intensity currently in effect for each building, while, at the same time, the same set of LCs were adopted (Repapis *et al.* 2006a, 2006b). For the purpose of the analysis, fourteen recorded base accelerograms were used. Inelastic dynamic analyses were performed for each accelerogram and for increasing acceleration intensity, until, in a step by step manner, the onset of first yield in any structural element and all failure LC were established. The corresponding peak absolute value of the base shear, the spectral acceleration or the *PGa* vs maximum absolute roof displacement from each analysis were obtained, in order to establish the IDA curve.

Similar to the SPO studies, the seismic performance of

each subject building was thereby quantified at both global and local levels. Among other response parameters, of interest were: i) the minimum elastic response spectrum acceleration intensity inducing first yield in any structural member, $(Sa)_y^{el}$, as well as the minimum elastic response spectrum acceleration intensity inducing conventional collapse, $(Sa)_c^{el}$, over all the input records; ii) the corresponding scaled record's maximum absolute values of the roof deformation δ_y and δ_c , respectively; iii) the evolution of peak local damage and demand indices, with record intensity, as delineated further on.

Assuming that the spectral amplification remains constant with intensity scaling, these response indices above allow for the establishment, using IDA, of the structure's available behaviour factor q and global ductility capacity μ , see Eq. (1) (following Salvitti and Elnashai 1996). This building system specific behaviour factor, obtained either through SPO or design spectrum compatible IDA procedures, together with the relevant information obtained (shear or ductile critical collapse involved, type and value of the minimum Damage Index, scatter of the results etc.), provides the necessary calibration for the code prescribed behaviour factor (also a function of building system), incorporating, in addition to inelastic single degree of freedom analysis predictions, further empirical and public safety consensus safety factors (Whittaker *et al.* 1999).

$$q = \frac{(Sa)_c^{el}}{(Sa)_y^{el}}, \quad \mu = \frac{\delta_c}{\delta_y} \quad (1)$$

For the establishment of conventional collapse and corresponding spectral intensity, for each record and building, the same local and global LCs were adopted as for the SPO studies (Repapis *et al.* 2006a, 2006b at local (member) and global (structural) level, and step by step checks were performed of the following:

i) exceedance of the plastic rotation capacity at the two column end critical regions, as a function of the current axial load in the member (LC designated as θ_{pl}); the plastic rotation capacity was obtained from the evaluation of the ultimate curvature supply, following fiber model analysis of the section and assuming a constant plastic hinge length equal to a) half the section effective depth or, b) following a more refined empirical expression, accounting also for improper joint anchorage of the reinforcement (Paulay and Priestley 1992), whichever governed (it should be noted at this point, that it is implicitly assumed that exceeding θ_{pl} in the beams does not trigger nominal failure);

ii) the member shear strength capacity (under the current axial load) exceeded the member strength, evaluated using the currently enforced design Code equations based on mean material properties and current axial load (LC designated V) and

iii) the peak absolute interstorey drift over the entire time history was less than 1.25% for all frames designed according to past generation of codes, or 2.5% for frame K60AEC8 (LC designated dr).

All the above IDA based LC verifications were obtained using the computer code *DrainExplorer* (Repapis 2002); the code organizes in a gradually increasing and iterative base input intensity search the entire IDA procedure, by post

processing each time history run in order to perform for each excitation increment all necessary LC interrogations, for yield and collapse identification.

Input to the program includes frame geometry, beam, column and wall critical region reinforcement details at each end and the base input time history, including its elastic response spectrum characteristics. Subsequent preprocessing evaluates the critical region cross-section characteristics for all members and establishes the structural model. Once the Drain-2DX (Prakash *et al.* 1993) building inelastic model and the design parameters of the structure (e.g., critical region local force and deformation capacities) are established, both SPO and IDA analysis procedures can subsequently be pursued, for the specified elastic design response spectrum and set of ground motion inputs.

Following the IDA option and for a given base accelerogram, the record PGa is automatically scaled and the corresponding time integration analysis is performed, assuming, in each case, a constant mass proportional Raleigh damping of 5%.

Post processing of the analysis follows, whereby the state of the structure (globally) and all the members (locally) are monitored in each analysis step, comparing, to the LCs defined above, in a step-by-step manner, roof and storey global deformations, local column plastic rotations and shear force demands. Once suitable intensity bounds are established, successive iterative refinements of time history solutions around the incipient yield and nominal collapse PGa , are followed, obtaining $(Sa)_y^{el}$ and $(Sa)_c^{el}$ and, thus, the structure's behaviour factor q and ductility capacity μ , and tracing the entire base shear versus roof drift IDA curve for the subject building and record. Management of the time history results using statistical techniques follows for the entire record set.

5. Comparison of SPO and IDA analyses results

The performance predictions (failure mode, behaviour factor, ductility and so on) using SPO analyses, by Repapis *et al.* (2006b), are compared herein with the corresponding predictions following the IDA methodology (Vamvatsikos and Cornell 2003). In the latter case, fourteen actually recorded accelerograms from recent earthquakes at sites within Greece and worldwide were used and the inelastic structural response of the subject frames is presented and compared. For each record, an IDA set of about twenty five nonlinear incremental dynamic analyses were performed, leading to a total of about 1700 nonlinear dynamic analyses, for the entire regular building inventory and fourteen record set adopted. The as recorded accelerogram histories are shown in Fig. 2, while their corresponding elastic response spectra are shown in Fig. 3; for comparison, the smoothed Elastic Design Response Spectrum (EDRS) in conformance to current EC8 (2004) requirements for zone I and II are also given, with PGa equal to 0.16 g and 0.24 g, respectively.

Consistent with design assumptions, all accelerogram histories used as base record for each IDA (subsequently referred to as the EDRS compatible record, herein), were

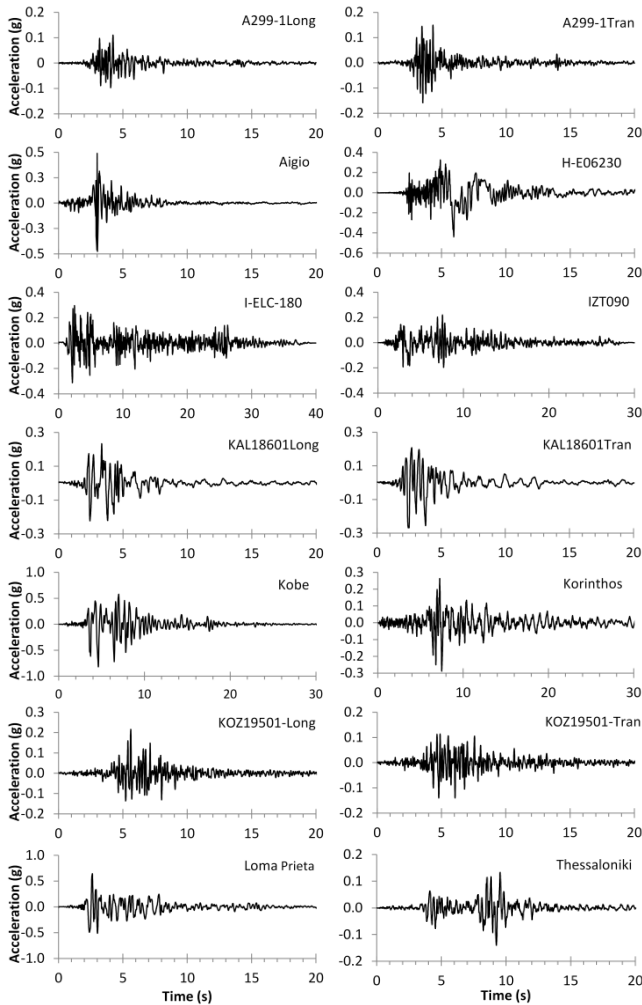


Fig. 2 Earthquake records

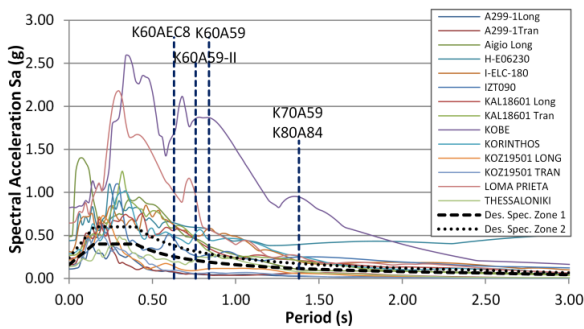


Fig. 3 Elastic response spectra of the as recorded accelerograms and building predominant periods

initially scaled so as to match the Velocity Spectrum Intensity (*VSI*) of the zone I EDRS of EC8 (2004). The recorded *PGA*, peak ground velocity (*PGV*), significant duration of the ground excitation (namely the time bounded by the 3% and 97% limits of the Arias Intensity) *t_d*, Arias Intensity (*AI*) and Velocity Spectrum Intensity (*VSI*) of the unscaled records are given in Table 2.

5.1 Response prediction based on SPO analysis

Inelastic SPO analyses were performed with uniform

Table 2 Ground motion characteristics of the records used

Record	Location & Date	<i>PGA</i> %g	<i>PGV</i> cm/sec	<i>VSI</i> cm	<i>AI</i> cm/sec	<i>t_d</i> sec
A299-1Long	Athens 1999	0.11	5.1	18.4	8.6	10.2
A299-1Tran	Athens 1999	0.16	7.1	21.1	14.5	8.4
Aigio Long	Aigio 1995	0.49	40.2	113.7	97.2	4.4
H-E06230	Imperial 1979	0.44	109.8	178.7	175.4	11.2
I-ELC-180	Imperial 1940	0.31	29.7	132.9	170.4	24.6
IZT090	Kocaeli 1999	0.22	29.8	112.3	81.3	16.6
KAL18601 Long	Kalamata 1986	0.23	30.9	106.9	54.2	6.1
KAL18601 Tran	Kalamata 1986	0.27	24.8	102.3	72.6	7.5
KOBE	Kobe 1995	0.82	81.4	417.4	839.0	10.8
KORINTHOS	Korinth 1981	0.29	23.5	123.6	85.3	16.4
KOZ19501 LONG	Kozani 1995	0.22	9.2	38.8	26.4	8.0
KOZ19501 TRAN	Kozani 1995	0.14	6.6	24.7	19.6	10.6
LOMA PRIETA	Loma Prieta 1989	0.64	55.1	179.6	323.8	10.2
THESSALONIKI	Thessaloniki 1978	0.14	11.4	51.8	17.2	8.7

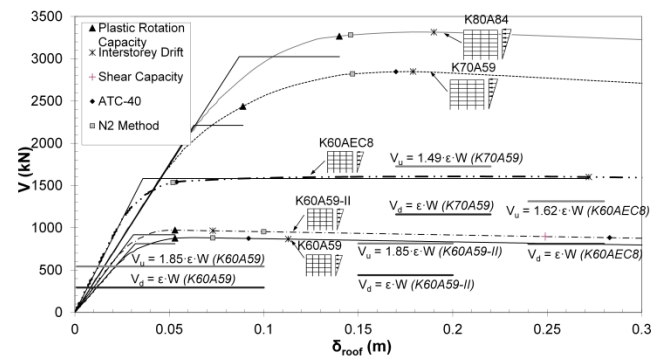


Fig. 4 Inelastic pushover characteristics of the frames considered (adopted from Repapis *et al.* 2006b)

and triangular distribution of lateral loads for both buildings (the latter results are taken from Repapis *et al.* 2006b). Regarding the local collapse criteria of a structural member, it was assumed that failure of the structure occurs only if a limit is exceeded in a column, assuming that failure of beams is less critical for failure characterization of the building. The predicted base shear-roof displacement characteristics of the investigated frames are shown in Fig. 4, together with an equal area bilinear approximation of the SPO curves for the estimation of the available ductility μ and behaviour factor q .

These curves give important properties of the structures, such as the initial stiffness, the maximum strength and yield resistance and the corresponding roof global displacement. At the same graph, the roof deformations at which the limit

Table 3 Results from the SPO analyses

Building	Profile	T_1 [sec]	V_{max} [KN]	Ω	μ	q	δ_c	δ_{CSM}	δ_{N2}	LC
K60A59	unif.	0.84	1012	1.86	1.85	2.57	6.0	7.5	6.5	θ_{pl}
	tr.		877	1.61	1.63	2.03	5.3	9.2	7.3	θ_{pl}
K60A59-II	unif.	0.76	1187	1.46	2.36	2.68	7.7	16.9	8.9	θ_{pl}
	tr.		973	1.19	1.72	1.77	5.3	28.3	10.0	θ_{pl}
K70A59	unif.	1.38	2772	1.47	1.25	1.44	7.1	13.6	12.4	θ_{pl}
	tr.		2436	1.30	1.40	1.55	8.9	16.9	14.7	θ_{pl}
K80A84	unif.	1.38	3455	1.97	1.40	2.03	10.9	12.6	12.4	θ_{pl}
	tr.		3266	1.73	1.61	2.21	14.0	12.8	14.6	θ_{pl}
K60AEC8	unif.	0.63	1807	1.37	5.83	4.80	19.4	6.7	4.6	dr
	tr.		1608	1.22	7.63	5.44	27.2	5.4	5.2	dr

state criteria considered are exceeded in any of the members are also denoted, together with the corresponding performance point demands following two performance point estimation methods, the Capacity Spectrum Method (CSM) proposed by ATC-40 (1996) and the N2 Method proposed by Fajfar (1999).

Furthermore, the design base shear V_d and the ultimate limit state (ULS) reference base shear V_u (equal to the allowable stress level design base shear multiplied by a material strength correction factor) for all frames are also shown, in order to quantify the overstrength of the structure. The interstorey drift limiting criterion is observed at large deformations and it is critical only for the frame designed to the modern design code. For existing buildings of *Groups 60, 70 and 80*, it is observed that the critical limit state criterion is the plastic hinge rotation capacity.

The results of SPO analysis are summarized in Table 3. In this Table, T_1 is the fundamental period of each structure, V_{max} is the maximum base shear attained by the structure, Ω is the overstrength, q is the available behaviour factor, μ is the ductility capacity of the equivalent bilinear system, δ_c is the roof drift at failure, δ_{CSM} and δ_{N2} are the target point demand following the CSM (ATC-40 1996) and N2 Method (Fajfar 1999), respectively and Limit Criterion is the controlling LC based on which δ_c was estimated.

The overstrength and the ductility of building K60A59 are 160% and 1.65 respectively and are higher than for building K70A59 (130% and 1.40), for triangular load distribution (Table 3). Building K80A84nw has higher overstrength and ductility from both K60A59 and K70A59 (173% and 1.61), because this structure is designed according to MOD84 (1984), which introduced end member confinement and the requirement for a joint capacity criterion (less strict than the one applied in the present codes), thereby increasing the structure's lateral resistance. Finally, building K60AEC8 has 122% overstrength and a ductility of 7.63, significantly higher than the buildings designed according to past generation of codes.

For the 60s and 70s buildings, the target displacement demands are higher than the maximum deformation capacity, though for different reasons in each case. For the building of the 80s closer demand and capacity values are obtained. In Table 3 it can be seen that the plastic rotation capacity LC, which governs in the buildings of the 60s and

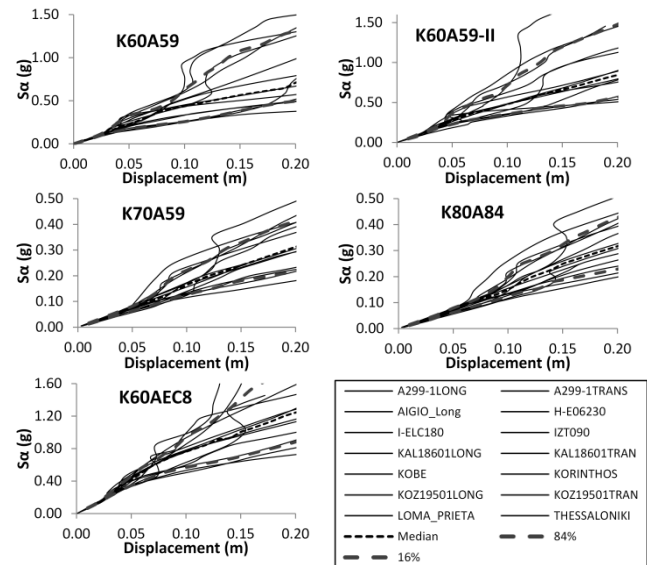


Fig. 5 IDA curves for irregular frames considered, for 14 records, median, 16% and 84%

70s, improves in the 80s frame as a result of detailing measures introduced in 1984. On the contrary, the capacity of K60AEC8, designed according to the current codes, is considerably higher than the target demand.

Building K60A59-II, designed for seismicity zone II, exhibits a higher lateral resistance compared to the K60A59. However, its lateral overstrength is not in proportion to the increase of design base shear seismic coefficient used for these two buildings: due to the fact that the design seismic force is based on allowable stresses and, also, is relatively low, an increase of 50% in the design base shear coefficient from 4% to 6% of the vertical loads results in a disproportionate increase of only 10% in V_{max} . On the other hand, its global ductility capacity is only slightly increased, but again, nowhere as much as the relative increase in the design base shear. Given, therefore, that the deformation capacities of both *Group 60* buildings is similar but the target displacement demand for zone II is almost doubled, the structure in zone II will be more critical from the point of view of seismic vulnerability and retrofit intervention priority than the one located in regions of seismicity zone I.

5.2 Response prediction based on IDA

IDA is performed for the investigated structures using the fourteen recorded base excitation histories described above. The maximum predicted total displacement during each nonlinear time history analysis is plotted against the spectral acceleration in Fig. 5. In these plots, the median IDA curves and the 16% and 84% fractiles of all the records are shown too. Buildings K70A59 and K80A84 exhibit the least amount of variability with input motion. Conventional collapse is checked using the same set of LC for each record. The global IDA results are shown in Table 4 and plotted in Fig. 6 for each record, while average, median, maximum and minimum predictions for the behaviour factor q , ductility capacity μ and the minimum predicted

Table 4 Behaviour factor, ductility and displacement at failure evaluated from Pushover and IDA analyses. Mean, median, minimum and maximum values from all the records

Record	K60A59 ($T=0.84$ sec)			K60A59-II ($T=0.76$ sec)			K70A59 ($T=1.38$ sec)			K80A84 ($T=1.38$ sec)			K60AEC8 ($T=0.63$ sec)		
	q	μ	δ_c (cm)	q	μ	δ_c (cm)	q	μ	δ_c (cm)	q	μ	δ_c (cm)	q	μ	δ_c (cm)
	Pushover-ortho	2.57	1.85	6.0	2.68	2.36	7.7	1.44	1.25	7.1	2.03	1.40	10.9	4.80	5.83
Pushover-trian	2.03	1.63	5.3	1.77	1.72	5.3	1.55	1.40	8.9	2.21	1.61	14.0	5.44	7.63	27.2
A299-1Long	3.47	3.85	4.8	3.31	4.38	4.4	2.97	2.97	2.80	2.8	5.88	6.42	11.36	20.89	26.9
A299-1Tran	2.95	2.43	2.8	3.78	2.94	3.4	1.43	1.43	1.42	3.2	5.47	4.62	14.41	12.44	15.7
Aigio Long	2.43	2.41	5.8	2.82	2.43	5.3	2.56	2.56	2.59	5.1	2.22	2.23	16.56	7.22	17.9
H-E06230	2.02	2.43	7.4	2.63	3.04	6.2	1.91	1.91	1.95	7.6	2.63	2.68	3.75	6.66	16.8
I-ELC-180	2.94	2.31	3.9	2.43	2.09	4.6	1.46	1.46	1.41	5.5	4.14	3.29	12.25	6.75	17.0
IZT090	2.16	1.89	4.7	1.86	1.92	3.9	1.91	1.91	1.92	6.6	1.38	1.39	5.58	5.90	15.9
KAL18601Long	2.43	1.70	4.3	2.43	2.04	4.4	1.46	1.46	1.39	5.0	2.44	2.17	7.53	6.50	16.4
KAL18601Tran	1.71	1.99	4.9	2.43	3.05	6.0	1.91	1.91	1.76	7.6	2.48	2.18	7.53	9.75	25.1
KOBE	2.43	2.35	5.8	2.98	2.91	6.1	1.91	1.91	1.59	5.4	2.67	1.88	4.75	7.21	18.8
KORINTHOS	2.43	2.03	4.7	2.91	2.10	4.3	2.53	2.53	2.11	7.5	3.90	2.70	8.08	6.78	17.2
KOZ19501Long	4.42	2.92	4.5	3.10	2.63	3.1	1.42	1.42	1.42	3.2	6.00	4.18	11.24	10.41	18.0
KOZ19501Tran	2.45	1.79	3.3	2.58	2.19	3.1	1.36	1.36	1.36	2.1	5.72	5.49	10.64	14.18	20.2
LOMA PRIETA	1.71	1.72	4.1	2.43	2.05	4.3	2.67	2.67	2.54	4.9	2.80	3.28	7.53	10.09	26.6
THESSALONIKI	3.11	2.09	5.0	2.96	2.15	4.4	2.18	2.18	2.23	7.2	2.40	2.21	9.13	7.80	16.5
Mean value	2.62	2.28	4.7	2.76	2.56	4.5	1.98	1.89	5.3	3.58	3.19	10.3	9.31	9.47	19.2
Median value	2.43	2.20	4.7	2.73	2.31	4.4	1.91	1.84	5.25	2.73	2.69	9.9	8.61	7.51	17.55
Min value	1.71	1.70	2.8	1.86	1.92	3.1	1.36	1.36	2.1	1.38	1.39	6.9	3.75	5.90	15.7
Max value	4.42	3.85	7.4	3.78	4.38	6.2	2.97	2.80	7.6	6.00	6.42	13.8	16.56	20.89	26.9
Standard deviation	0.72	0.57	1.1	0.47	0.67	1.0	0.53	0.50	1.9	1.59	1.47	2.0	4.80	5.83	19.4
Coef. of variation	0.28	0.25	0.24	0.17	0.26	0.23	0.27	0.26	0.36	0.44	0.46	0.19	5.44	7.63	27.2

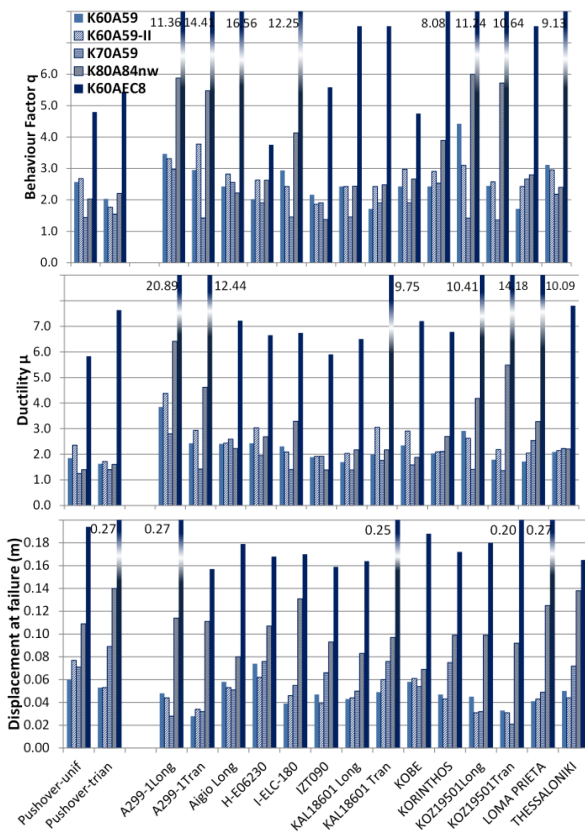


Fig. 6 Behaviour factor, ductility and displacement at failure evaluated from SPO and IDA analyses. (Building K60AEC8 results out of vertical scale)

roof drift at collapse (δ_c) are compared to the static pushover results. In all cases there is a wide scatter in the global demand indices (Table 4 and Fig. 6).

From comparison between the SPO and IDA predictions (Table 4 and Fig. 6) it can be seen that the q factor, ductility capacity and roof displacement at failure predicted by the dynamic analyses exhibit a wide variability around the mean values. In general, mean values for q factor and μ evaluated with IDAs are relatively higher compared to the values evaluated with SPO analysis. However, the values evaluated from SPO analysis are included between the minimum and maximum values from IDAs. Building K60AEC8 designed according to EC8 exhibits considerably higher mean values for q and μ , as expected. Moreover, building K60A59-II, designed in zone II, exhibits higher mean values for most records than K60A59, designed in zone I. Building K70A59 with the bigger spans and more storeys has the smaller values, while building K80A84, designed to MOD84 (1984), has higher values and the best behaviour compared to the previous buildings. Moreover, building K80A84 consistently depicts higher yield and collapse roof deformations (almost double), compared to the previous generation buildings, in all types of earthquake excitation. As expected, building K60AEC8, designed to current design codes, has significantly higher values from all other buildings.

The form of failure defining q and μ for the structural systems considered is not the same among different records while, in cases, it varies from the controlling LC under the SPO prediction. In some cases the failure form changes for

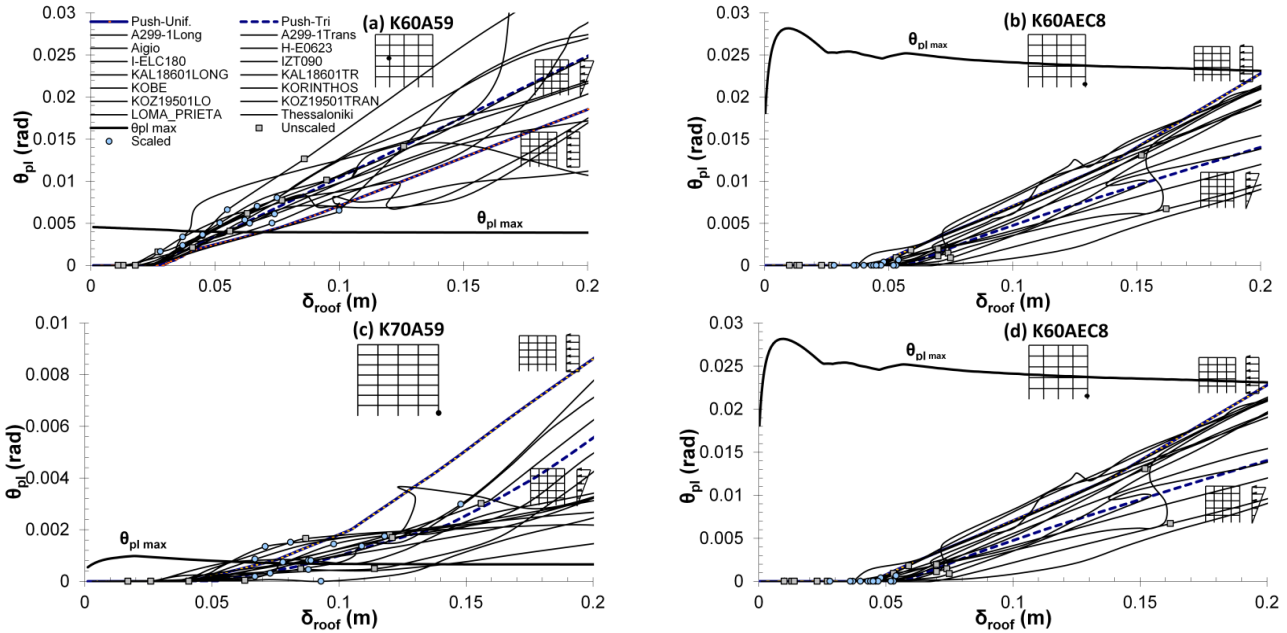


Fig. 7 Plastic hinge rotation of the top of a perimeter column of the 3rd storey. Building (a) K60A59, (b) K60AEC8, (c) K70A59 and (d) K80A84

the same building as the earthquake base input gradually increases, yet in some systems it remains consistently the same. Building K60A59 exhibits plastic rotational capacity (θ_{pl}) failure consistently for all PGa 's for the KAL18601LONG record. For the same record, building K70A59 exhibits plastic rotational capacity (θ_{pl}) failure for lower PGa values and shear (V) failure for higher PGa values. For building K80A84, critical limit states switch between plastic rotation capacity (θ_{pl}) and interstorey drift (dr), as the same earthquake base input gradually increases.

In Fig. 7, the plastic hinge rotation at the top of a perimeter column at the 3rd storey of building K60A59 versus roof displacement is shown, for the fourteen IDAs, together with the curves evaluated from SPO analyses with uniform and triangular distribution of lateral forces; for comparison, the corresponding capacity ($\theta_{pl\ max}$) is also given, for the latter SPO analysis case. The top section of a perimeter column of the 3rd storey of building K60A59 and the bottom section of a corner column at the base of buildings K60AEC8, K70A59 and K80A84 are selected (note that the members shown were the critical members governing nominal failure in the SPO analyses). In addition to these, failure points from dynamic analyses under the EDRS and the unscaled record are also shown. Plastic rotation demands exhibit wide scattering with minimum scatter observed for building K60AEC8. The columns of buildings K60A59 and K70A59 examined have no plastic hinge rotation for some unscaled records while, for other excitations, the plastic rotation exceeds by a large proportion the capacity of the member. The same is observed for the records scaled to EDRS, showing that for most records the capacity of the member is exceeded. Improvement in this behaviour is observed for building K80A84, for which the plastic rotation of the examined member under the EDRS records is smaller than the member's capacity for most cases. Finally, for building

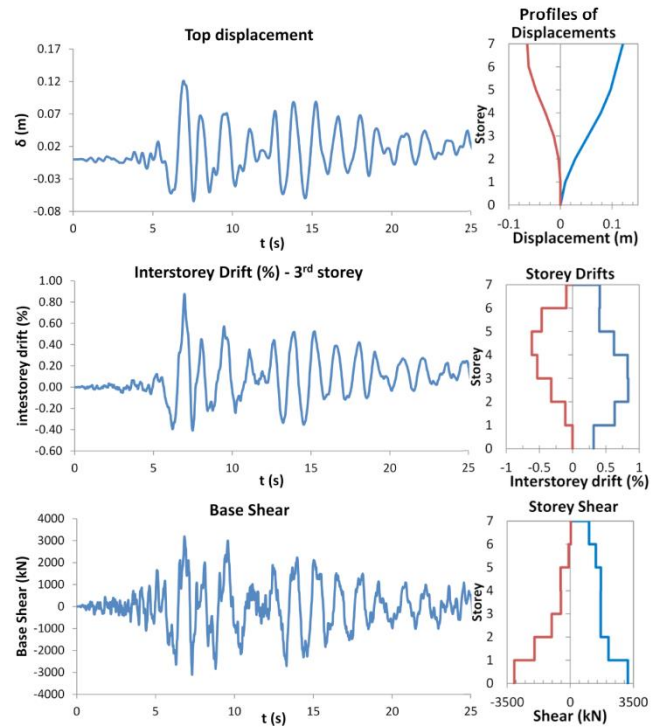


Fig. 8 Time-histories and profiles for the KORINTHOS record (K70A59 building)

K60AEC8, the plastic rotation of the member for both unscaled and scaled records is significantly smaller than the capacity of the member, confirming the improved behaviour of buildings designed to modern codes. For this building it is also observed that the scatter of the results is quite smaller than for all other buildings.

Time histories for displacement, interstorey drift and shear forces at each storey and their profiles, are evaluated for each record at every step of the analysis. In Fig. 8 time

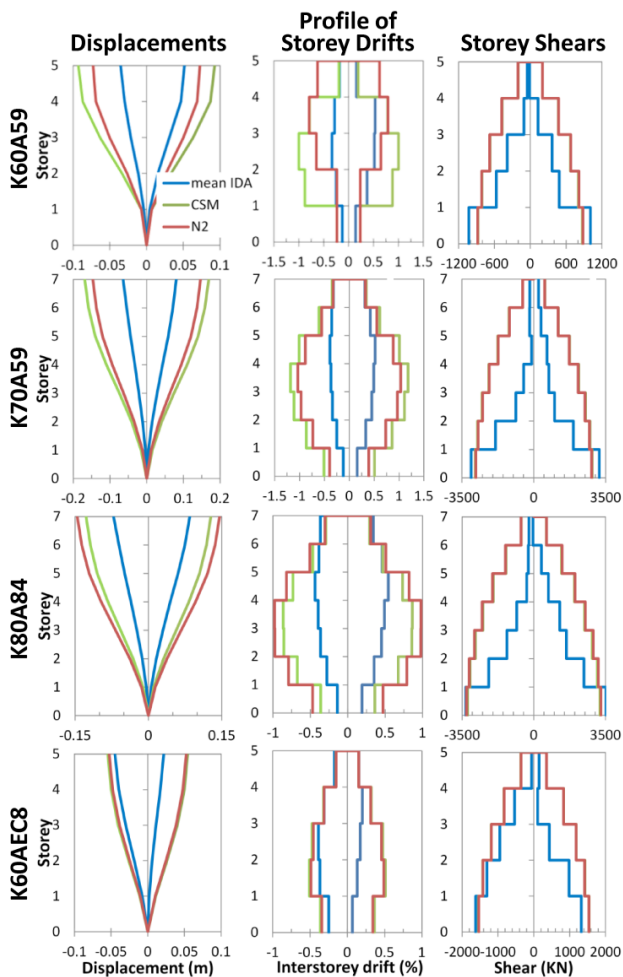


Fig. 9 Profiles of storey displacements, interstorey drifts and shear forces from SPO and IDA analyses

histories for top displacement, interstorey drift of the 3rd storey and base shear are presented for building K70A59 under the Korinthos record. Profiles of these response parameters are presented in the same figure at the times of maximum displacement and maximum base shear. It can be seen that for this record, interstorey drift is maximum at the 3rd storey.

In Fig. 9 the profiles of storey displacements, interstorey drifts and shear forces are presented. Median values from nonlinear dynamic analyses, performed with the records scaled to EDRS, are compared with the values from SPO analysis. Profiles for SPO analysis are shown when the building is deformed at the target displacements obtained using the CSM and N2 methods. It can be seen that nonlinear static methods overestimate the displacements, interstorey drifts and shear forces. There are differences among the two static evaluation techniques in the distribution of storey displacements and interstorey drifts, while distribution of shear forces is almost identical (the two methods predictions overlap in the Figure). The results of N2 method seem to be closer to the nonlinear dynamic analysis but with significant differences. The building of the 70s (K70A59) exhibits the larger displacements and interstorey drifts, while the building designed according to the current design code (K60AEC8), the smallest.

In Fig. 10 the plastic hinge distributions are shown for dynamic analysis of building K60A59, K60AEC8, K70A59 and K80A84, for the unscaled KORINTHOS record, at the time when the maximum interstorey drift was attained in each case. In the same figure ductility rotation demands are shown near each plastic hinge. Furthermore, energy absorption for beams and columns along the height of the building is plotted aside of the hinge plots, at the same time. For building K60A59 of the 60s, at the time when the maximum interstorey drift was attained, the energy absorption and the ductility rotation demands are maximum at the 3rd storey, where interstorey drift is also maximum. From the plastic hinge distribution it can be seen that a soft storey mechanism is created in the 3rd and 4th storey and a lot of members fail. More than 30% of the total energy is absorbed by the columns of the 3rd storey while 19% and 17% is absorbed by the columns of the 2nd and 4th storeys, respectively. Beams at the two lower storeys absorb only 16% of the total energy. On the contrary, for building K60AEC8 designed to modern codes, plastic hinges occur mainly at the beams and thus energy absorption is concentrated mainly to the beams. Moreover, energy absorption is better distributed along the height of the structure, while only 25% is absorbed by the columns of the two lower storeys.

On the other hand, buildings K70A59 of the 70s and K80A84 of the 80s, having wider bay sizes, absorb inelastic energy primarily by flexure in the beams, despite the fact that only for the buildings of *Group 80* a capacity design was actually enforced by the design code, albeit using allowable stress quantities. Plastic hinges are observed mainly to the beams and energy is uniformly distributed to the beams along the height of the building (Fig. 10). Local ductility rotation demands are higher, while capacity is lower, for building K70A59 for which some members fail.

In Fig. 11 the peak roof displacements of all the buildings subjected to the fourteen records are presented. These displacements correspond to four levels of intensity for each record. The values represent (i) the displacement from dynamic analysis with the record under minimum intensity that causes 1st yield to any member of the structure, (ii) the displacement from analysis that causes 1st failure, (iii) the displacement with the record scaled to design spectrum and (iv) the displacement with the natural (unscaled) record. It can be seen that in most cases of the buildings of the 60s and 70s, the maximum displacement with the minimum record that causes failure is smaller than the maximum displacement obtained from dynamic analysis with the scaled record for all IDAs. For building of the 70s failure exhibits worse behaviour compared to the building of the 60s. Building K60A59-II (seismicity zone II) has similar behaviour with building K60A59 (seismicity zone I). Building K80A84 exhibits an improved behaviour since for many records failure displacement is higher than the maximum displacement obtained from dynamic analysis with the unscaled record. Finally, building K60AEC8 designed to modern earthquake design codes, has the best behaviour and, for the entire set of records, the failure displacement is significantly higher than the maximum displacement obtained from dynamic analysis with both scaled and unscaled records.

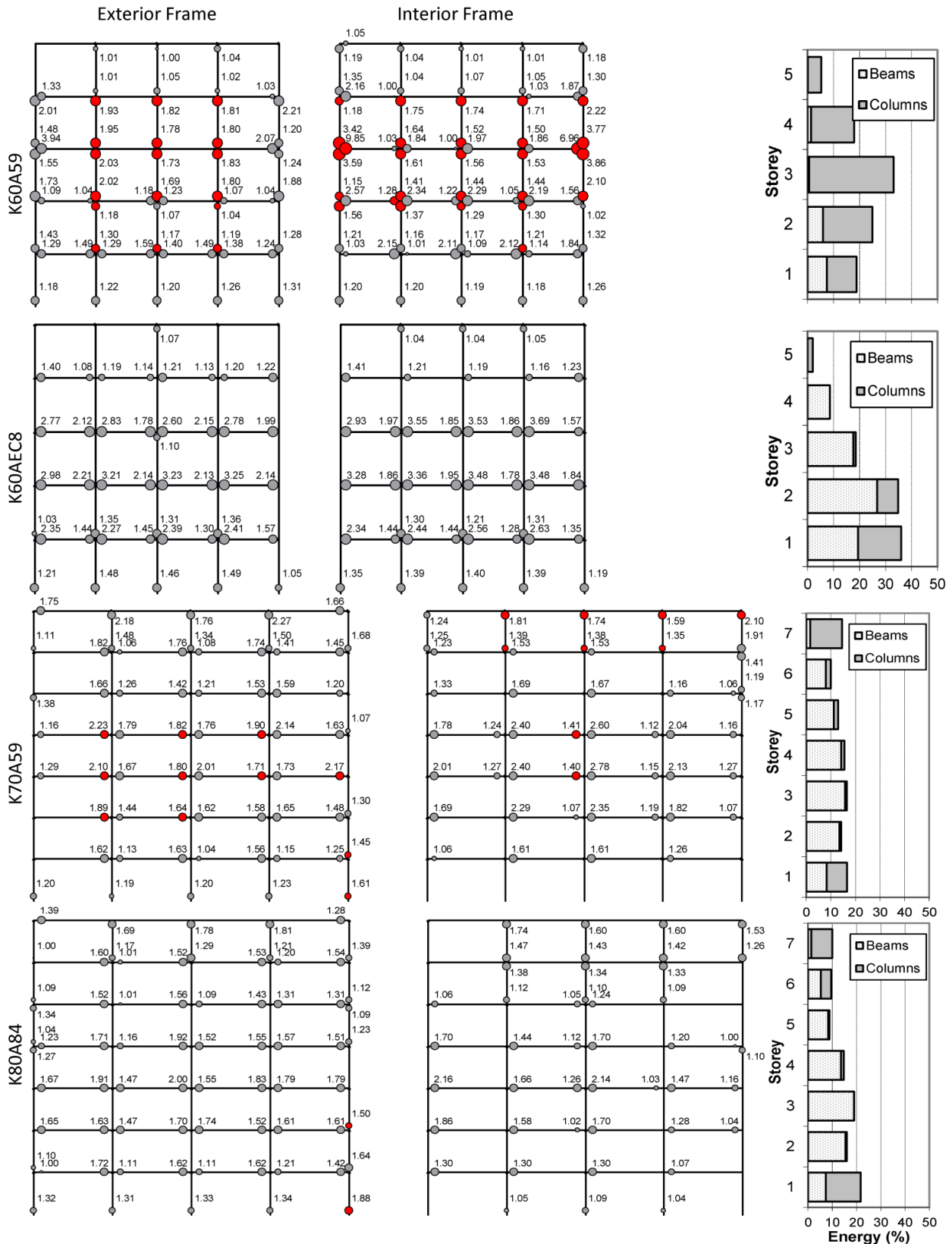


Fig. 10 Plastic hinge distribution, ductility rotation demands and energy absorption for the step at maximum drift. KORINTHOS record. Red plastic hinges have failed

These results are summarized in Fig. 12, in which the median IDA curves of all the records are compared for the five buildings. In the same figure, the median deformation

points from dynamic analysis of the records set at yield and failure, scaled to EDRS and unscaled as recorded, are also shown. The building of *Group 60* for seismic zone II

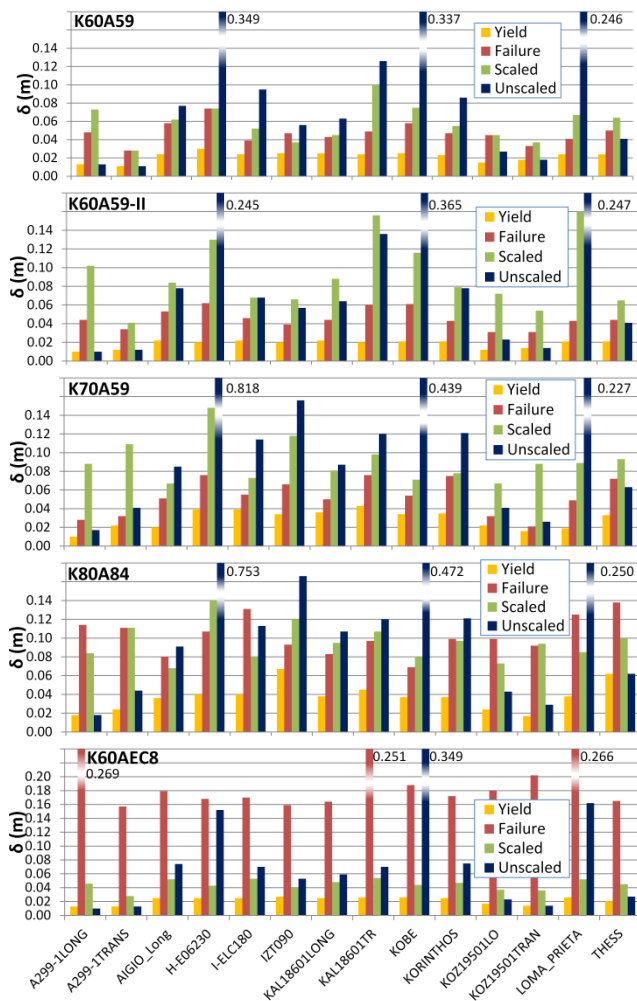


Fig. 11 Displacements from IDA analysis for 14 records. Values for yield, failure, the scaled record to the design spectrum and the unscaled record. (Building K60AEC8 results out of vertical scale)

(K60A59-II) exhibits higher base shear capacity than the building of zone I (K60A59), while for both buildings the maximum deformation capacity is similar and smaller than the demand (for the EDRS records scaled to the design spectrum). Moreover, the base shear capacity of the same building but designed according to modern codes (K60AEC8) is higher and its maximum deformation capacity is significantly larger than the demand. The base shear capacity is also higher for the buildings of the 70s and 80s (K70A59 and K80A84), since these are buildings with wider spans and more storeys. The maximum deformation capacity of building K70A59 is quite smaller than the demand, while for building K80A84 the median maximum deformation capacity exceeds slightly the demand, showing an improved behaviour. For all cases, the median points of the unscaled records correspond to larger deformation than the points of the records scaled to the design spectrum.

In Fig. 13 SPO predictions with triangular distribution of lateral loads are compared to the median IDA predictions. Median IDA curves in terms of maximum base shear vs maximum roof deformation are shown in Fig. 13, with indication of the median level at failure and excitation

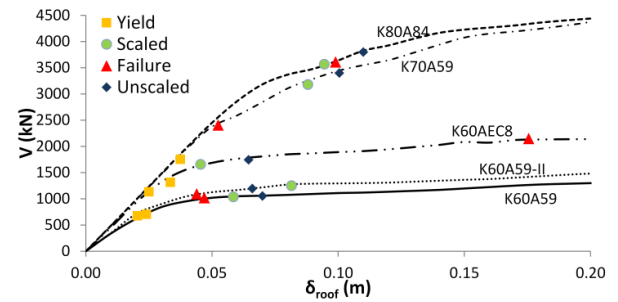


Fig. 12 Median IDA curves for bare frames designed according to different codes

demand with the scaled record. Similarly, in SPO curves, target and failure displacements are also depicted. Target displacements were evaluated according to the CSM and N2 methods. For all the cases the base shear capacity of the IDA curves was larger than the SPO curves, with the building of the 70s (K70A59) showing the larger increase.

The target roof displacement for the buildings of the 60s (zone I) varies from 7.3 to 9.2 cm (Table 3), evaluated from SPO analysis with triangular distribution of lateral loads according to N2 method and CSM method, while the median value from nonlinear dynamic analyses using records scaled to the EDRS is 5.9 cm. Similarly, for building K60AEC8 designed to modern codes, the target displacement from SPO is 5.2 to 5.4 cm and from IDA is 4.5 cm. For buildings of the 70s and 80s (K70A59 and K80A84) target displacement from pushover analysis varies from 16.9 to 12.8 cm, while the demand from IDA varies from 8.8 to 9.5 cm.

From the SPO and IDA comparisons, it is evident that for all cases considered, the nonlinear static prediction methods overestimate the target displacement demand as compared to the median peak roof deformation from IDA. As it is shown in Fig. 13, the seismic demand evaluated with SPO analyses is larger than the demand evaluated using IDA. For the buildings of the 60s (zone I) and the 70s, the seismic demand is higher than the maximum deformation capacity of these structures. For building K60A59-II of the 60s designed in zone II, the deformation capacity is similar to the one of the building of zone I, while the target displacement demand is significantly increased similar to the performance prediction results of SPO analysis discussed in 5.1, confirming therefore, using IDA as well, that buildings of zone II are seismically more vulnerable. The building of *Group 80* exhibits an improved behaviour, since the median demanded deformation from the IDA analyses is lower than the maximum deformation capacity. For this building, the demand is slightly higher than the maximum deformation capacity when evaluated with SPO analysis. Finally, and as expected, for building K60AEC8 designed according to current codes the maximum deformation capacity is significantly higher than the seismic demand.

6. Conclusions

Analytical predictions of the performance of existing

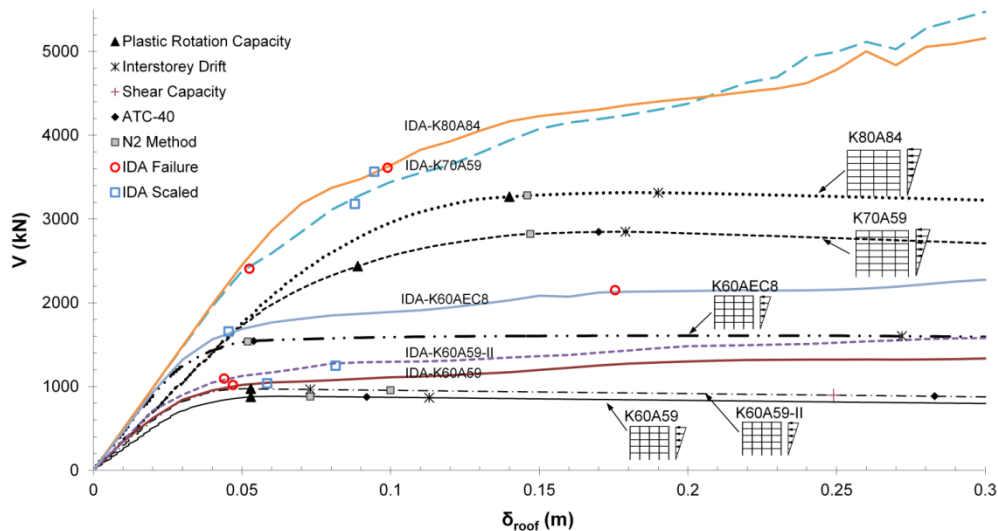


Fig. 13 Median IDA curves for bare frames with different form of irregularity

medium rise RC structures are evaluated. Investigated structures were designed and constructed since 1960 in Greece, according to previous seismic design codes in effect during these periods. The analyses are based on Incremental Dynamic Analyses and are compared to previous analysis assessments of the seismic performance of these structures based on static methods. Based on the analysis results and the relative comparisons, the following are concluded.

6.1 Use of IDA for seismic performance prediction

- The behaviour factor q , ductility capacity and roof displacement at failure predicted by the dynamic analyses exhibit a wide variability around the mean values. In general, mean values for the behaviour factor and ductility capacity evaluated with IDAs are higher compared to the values evaluated with pushover analysis. However, the values evaluated from pushover analysis are included between the minimum and maximum values from IDAs.

- The roof drift (δ_c) at failure obtained from the IDA is consistently less than the value predicted by SPO analysis, using a triangular lateral load distribution.

- Unlike SPO predictions, which gave in all cases that the reduced flexural capacity of the columns (rather than shear strength) governed nominal failure, critical performance using IDA procedures established that a) shear critical brittle mechanisms may also occur for certain input frequency contents and b) the flexural collapse mechanism, when mobilized, was different to SPO, penalizing further column demands.

- One should note however that the estimation of expected inelastic performance is sensitive to a number of analysis parameters, namely the model, the refinement of the failure criteria adopted and the performance point estimation method. Also, the assumed rigidity of the beam-column joints may not be totally correct for existing structures with relatively small member dimensions and inadequate anchorage. These assumptions need to be examined further with more reliable analytical models.

6.2 Comparison of different building generations

- Buildings of the 60s have small bay sizes. Global ductility strongly depends on bay width, with the stiffer buildings, having smaller bay sizes, exhibiting higher ductility values compared to buildings of the 70s.

- Building of the 80s has higher overstrength and ductility compared to the buildings of the 60s and 70s, because this structure was designed according to MOD84 (1984), which introduced end member confinement and the requirement for a joint capacity criterion. As expected, building designed to modern codes has significantly increased ductility capacity the best behaviour.

- For building of the 60s most of the energy is absorbed by the columns and a soft storey mechanism is observed at the middle storeys. On the contrary, buildings K70A59 and K80A59, having wider bay sizes, absorb flexural inelastic energy primarily in the beams, although only for buildings of the 80s a capacity design was actually considered by the design code. For these buildings, plastic hinges are observed mainly to the beams and energy is uniformly distributed to the beams along the height of the building. As expected, for the building designed to modern codes the plastic hinges occur mainly at the beams and thus energy absorption is concentrated to the beams.

- Maximum deformation capacity is smaller than the demand for buildings of the 60s and 70s. For seismicity zone II building, the capacity is similar to zone I, while the demand almost doubles, making this building critical from the point of view of seismic vulnerability and retrofit intervention priority than the one located in regions of seismicity I. An improved behaviour is observed for building of the 80s for which maximum deformation capacity is a little higher than the demand. Finally for building designed to the modern codes, maximum deformation capacity is significantly higher than the demand. Similar results were obtained from pushover analyses too.

References

- Anagnostopoulos, S. and Lekidis, V. (1986), "Seismic design based on the new provisions of the design code: application examples, instructions and parametric investigations", ITSAK, Thessaloniki. (in Greek)
- Applied Technology Council (1996), "Seismic evaluation and retrofit of reinforced concrete buildings", Report ATC 40 / SSC 96-01, Palo Alto.
- Bala, I.E., Crowley, H., Pinho, R. and Gülay, F.G. (2008), "Detailed assessment of structural characteristics of Turkish RC building stock for loss assessment models", *Soil Dyn. Earthq. Eng.*, **28**, 914-932.
- Benavent-Climent, A. and Zahran, R. (2010), "Seismic evaluation of existing RC frames with wide beams using an energy-based approach", *Earthq. Struct.*, **1**(1), 93-108.
- Borzi, B., Vona, M., Masi, A., Pinho, R. and Pola, D.C. (2013), "Seismic demand estimation of RC frame buildings based on simplified and nonlinear dynamic analyses", *Earthq. Struct.*, **4**(2), 157-179.
- Bracci, J.M., Reinhorn, A.M. and Mander, J.B. (1995), "Seismic resistance of reinforced concrete frame structures designed for gravity loads: performance of structural system", *ACI Struct. J.*, **92**(5), 597-609.
- De Stefano, M., Tanganelli, M. and Viti, S. (2013), "On the variability of concrete strength as a source of irregularity in elevation for existing RC buildings: a case study", *Bull. Earthq. Eng.*, **11**, 1711-1726.
- Decanini, L., de Sortis, A., Goretti, A., Liberatore, L., Mollaioli, F. and Bazzurro, P. (2004), "Performance of reinforced concrete buildings during the 2002 Molise, Italy, earthquake", *Earthq. Spectra*, **20**(1), 221-256.
- EAK (2000), Ministry of Environment, Planning and Public Works, "Greek Earthquake Resistant Design Code", Decree 2184B/20.12.1999, 1154B/12.8.2003, Athens, Greece. (in Greek)
- EC1 (2002), European Committee for Standardization, EN-1991, Eurocode No. 1, "Actions on Structures", Brussels.
- EC2 (2004), European Committee for Standardization, EN-1992-1-1, "Eurocode No. 2, Design of Concrete Structures, Part 1: General Rules and Rules for Buildings", Brussels.
- EC8 (2004), European Committee for Standardization, EN-1998-1, Eurocode No. 8, "Design of Structures for Earthquake Resistance, Part 1: General Rules, Seismic Actions and Rules for Buildings and National Annex", Brussels.
- Ehlers, G. (1960), "Beton-Kalender. Taschenbuch für Beton- und Stahlbetonbau sowie die verwandten Fächer", **2**, Verlag Von Wilhelm Ernst & Sohn, Berlin. (in German)
- EKOS (2000), Ministry of Public Works, "Greek Code for Design of Concrete Works", Decree 1329B/6.11.2000, Athens, Greece. (in Greek)
- Eleftheriadou, A. and Karabinis, A. (2012), "Seismic vulnerability assessment of buildings based on damage data after a near field earthquake (7 September 1999 Athens-Greece)", *Earthq. Struct.*, **3**(2), 117-140.
- Fajfar, P. (1999), "Capacity spectrum method based on inelastic demand spectra", *Earthq. Eng. Struct. Dyn.*, **28**, 979-993.
- Favvata, M.J., Naoum, M.C. and Karayannis, C.G. (2013), "Limit states of RC structures with first floor irregularities", *Struct. Eng. Mech.*, **47**(6), 791-818.
- FEMA (2000), "Prestandard and commentary for the seismic rehabilitation of buildings (FEMA 356)", Federal Emergency Management Agency, Washington (DC).
- Ghobarah, A., Aly, N.M. and El-Attar, M. (1998), "Seismic reliability assessment of existing reinforced concrete buildings", *J. Earthq. Eng.*, **2**(4), 569-592.
- Hueste, M.B.D. and Bai, J.W. (2007), "Seismic retrofit of a reinforced concrete flat-slab structure: Part I-seismic performance evaluation", *Eng. Struct.*, **29**, 1165-1177.
- IAEE (2008), "Regulations for seismic design; A world list-2008", <http://www.iaee.or.jp/>
- Iervolino, I., Manfredi, G., Polese, M., Verderame, G.M. and Fabbrocino, G. (2007), "Seismic risk of R.C. building classes", *Eng. Struct.*, **29**, 813-820.
- Krawinkler, H. and Seneviratna, G.D.P.K. (1998), "Pros and cons of a pushover analysis of seismic performance evaluation", *Eng. Struct.*, **20**(4-6), 452-464.
- La Brusco, A., Mariani V., Tanganelli M., Viti S. and De Stefano M., (2015), "Seismic assessment of a real RC asymmetric hospital building according to NTC 2008 analysis methods", *Bulletin of Earthquake Engineering*, **13**, 2973-2994.
- LC45 (1945), Ministry of Public Works, "Greek Loadings Code", G.G. 325 A 31.12.45, Athens, Greece. (in Greek)
- Lima, C., De Stefano, G. and Martinelli, E. (2014), "Seismic response of masonry infilled RC frames: practice-oriented models and open issues", *Earthq. Struct.*, **6**(4), 409-436.
- Lynch, K.P., Rowe, K.L. and Liel, A.B. (2011), "Seismic performance of reinforced concrete frame buildings in Southern California", *Earthq. Spectra*, **27**(2), 399-418.
- Mehani, Y., Bechtoula, H., Kibboua, A. and Naili, M. (2013), "Assessment of seismic fragility curves for existing RC buildings in Algiers after the 2003 Boumerdes earthquake", *Struct. Eng. Mech.*, **46**(6), 791-808.
- MOD84 (1984), Ministry of Public Works, "Amendments and Additions to the RD of 26/2/59", Decree 239B/6-4-1984, Athens, Greece. (in Greek)
- Mwafy, A.M. and Elnashai, A.S. (2001), "Static pushover versus dynamic collapse analysis of RC buildings", *Eng. Struct.*, **23**, 407-424.
- NEAK (1995), Ministry of Environment, Planning and Public Works, "Greek Earthquake Resistant Design Code", Decree 534B/20-6-1995, Athens, Greece, (in Greek)
- NEKOS (1991), Ministry of Public Works, "New Greek Code for Design of Concrete Works", Decree 1068B/31-12-1991, Athens, Greece. (in Greek)
- Nguyen, X.H. and Nguyen, H.C. (2016), "Seismic behavior of non-seismically designed reinforced concrete frame structure", *Earthq. Struct.*, **11**(2), 281-295.
- Ni, P. (2014), "Seismic assessment and retrofitting of existing structure based on nonlinear static analysis", *Struct. Eng. Mech.*, **49**(5), 631-644.
- Paulay, T. and Priestley, M.N.J. (1992), *Seismic Design of Reinforced Concrete and Masonry Buildings*, John Wiley & Sons, Inc., New York.
- Pianigiani, M. and Mariani, V. (2017), "Sensitivity study on the discretionary numerical model assumptions in the seismic assessment of existing buildings", *Soil Dyn. Earthq. Eng.*, **98**, 155-165.
- Prakash, V., Powell, G.H. and Campbell, S. (1993), "Drain-2DX: Base program description and user guide", Version 1.10, Report No. UCB/SEMM-93/17, Dept. of Civil and Environmental Engineering, University of California, Berkeley.
- RD59 (1959), Ministry of Public Works, "Earthquake design regulation of building works", Royal Decree 26/2/59, Decree 36A/26/2/59, Greece, (in Greek)
- Repapis, C. (2002), "DrainExplorer, a Drain-2DX post-processor program", Reinforced Concrete Laboratory, Dept. of Civil Engineering, National Technical University of Athens, Greece.
- Repapis, C., Vintzileou, E. and Zeris, C. (2006a), "Evaluation of the seismic performance of existing RC buildings: I. Suggested methodology", *J. Earthq. Eng.*, **10**(2), 265-287.
- Repapis, C., Zeris, C. and Vintzileou, E. (2006b), "Evaluation of the seismic performance of existing RC buildings: II. A case study for regular and irregular buildings", *J. Earthq. Eng.*,

- 10(3), 429-452.
- Salvitti, L.M. and Elnashai, A.S. (1996), "Evaluation of Behaviour Factors for RC buildings by nonlinear dynamic analysis", *Proceedings of the 11th World Conference on Earthquake Engineering*, Acapulco, Mexico.
- Tanganelli, M., Viti, S., Mariani, V. and Pianigiani, M. (2017), "Seismic assessment of existing RC buildings under alternative ground motion ensembles compatible to EC8 and NTC 2008", *Bull. Earthq. Eng.*, **15**, 1375-1396.
- Thermou, G.E. and Pantazopoulou, S.J. (2011), "Assessment indices for the seismic vulnerability of existing R.C. buildings", *Earthq. Eng. Struct. Dyn.*, **40**(3), 293-313.
- Vamvatsikos, D. and Cornell, C.A. (2003), "Applied incremental dynamic analysis", *Earthq. Spectra*, **20**(2), 525-533.
- Whittaker, A., Hart, G. and Rojahn, C. (1999), "Seismic response modification factors", *J. Struct. Eng.*, **125**(4), 438-444.
- Zeris, C., Giannitsas, P., Alexandropoulos, K. and Vamvatsikos, D. (2006), "Inelastic modeling sensitivity of the predicted seismic performance of an existing RC building", *Proceedings of the 13th European Conference of Earthquake Engineering*, Geneva, Switzerland.
- Zeris, C., Vamvatsikos, D., Giannitsas, P. and Alexandropoulos, K. (2007), "Impact of FE modeling in the seismic performance prediction of existing RC buildings", *ECCOMAS Thematic Conference on Computational Methods in Structural Dynamics and Earthquake Engineering, COMPDYN 2007*, Rethymnon.

AT

Appendix A. Reinforcement detailing of beams and columns

The cross-sections and the reinforcement detailing of beams and columns for all the buildings are presented in Sections A.1 and A.2, respectively. Buildings are regular with double symmetry (Fig. 14) so the cross-sections and the reinforcement of only two beams and three columns of an exterior and interior frame are presented.

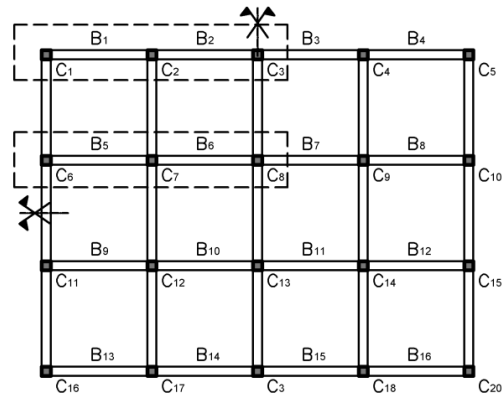
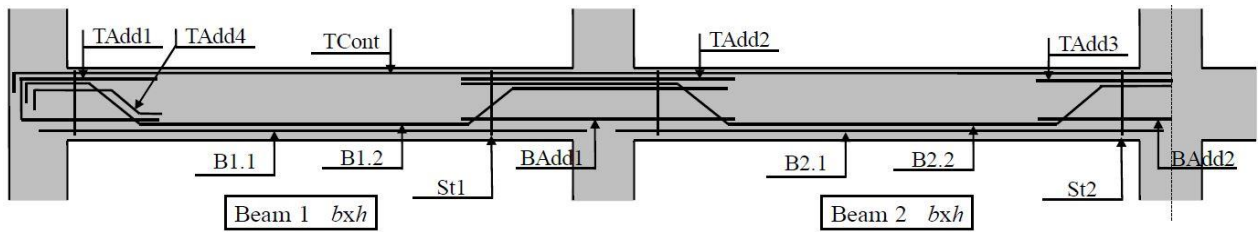


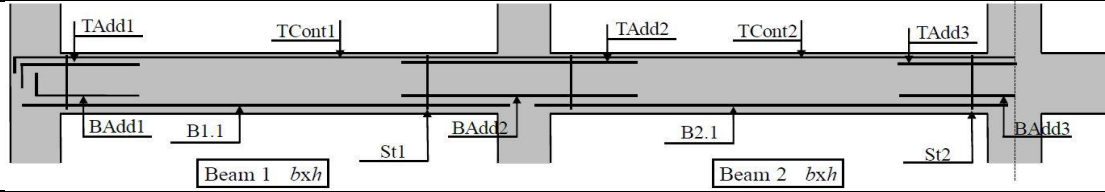
Fig. 14 Key plan

A.1 Beam schedules



	Floor	Frame	b(mm)	h(mm)	B1.1	B1.2	B2.1	B2.2	Badd1	Badd2	Tcont	Tadd1	Tadd2	Tadd3	Tadd4	St1	St2
K60A59	1	Ext	200	500	2d12	2d12	2d10	2d10	-	-	2d10	3d12	-	-	-	d8@300	d8@300
	1	Int	200	500	2d10	3d10	2d10	2d10	-	-	2d10	2d14	-	-	-	d8@300	d8@300
	2	Ext	200	500	2d10	3d10	2d10	2d10	-	-	2d10	5d10	-	-	-	d8@300	d8@300
	2	Int	200	500	2d10	3d10	2d10	2d10	-	-	2d10	2d12	-	-	-	d8@300	d8@300
	3	Ext	200	500	2d10	3d10	2d10	2d10	-	-	2d10	2d14	-	-	-	d8@300	d8@300
	3	Int	200	500	2d10	3d10	2d10	2d10	-	-	2d10	1d12	-	-	-	d8@300	d8@300
	4	Ext	200	500	2d10	2d10	2d10	2d10	-	-	2d10	2d12	-	-	-	d8@300	d8@300
	4	Int	200	500	2d10	2d10	2d10	2d10	-	-	2d10	1d10	-	-	-	d8@300	d8@300
	5	Ext	200	500	2d10	2d10	2d10	2d10	-	-	2d10	-	-	-	-	d8@300	d8@300
	5	Int	200	500	2d10	2d10	2d10	2d10	-	-	2d10	-	-	-	-	d8@300	d8@300
K60A59-II	1	Ext	200	500	2d14	2d14	2d10	2d10	-	-	2d10	5d10	-	-	-	d8@300	d8@300
	1	Int	200	500	2d14	2d14	2d10	2d10	-	-	2d10	3d14	-	-	-	d8@300	d8@300
	2	Ext	200	500	2d10	3d10	2d10	2d10	-	-	2d10	5d10	-	-	-	d8@300	d8@300
	2	Int	200	500	2d12	2d12	2d10	2d10	-	-	2d10	4d12	-	-	-	d8@300	d8@300
	3	Ext	200	500	2d10	3d10	2d10	2d10	-	-	2d10	5d10	-	-	-	d8@300	d8@300
	3	Int	200	500	2d10	3d10	2d10	2d10	-	-	2d10	2d14	-	-	-	d8@300	d8@300
	4	Ext	200	500	2d10	2d10	2d10	2d10	-	-	2d10	2d14	-	-	-	d8@300	d8@300
	4	Int	200	500	2d10	2d10	2d10	2d10	-	-	2d10	1d14	-	-	-	d8@300	d8@300
	5	Ext	200	500	2d10	2d10	2d10	2d10	-	-	2d10	-	-	-	-	d8@300	d8@300
	5	Int	200	500	2d10	2d10	2d10	2d10	-	-	2d10	-	-	-	-	d8@300	d8@300
K70A59	1	Ext	250	500	2d12	2d12	2d10	3d10	1d10	1d10	2d10	5d12	2d12	2d12	-	d8@300	d8@300
	1	Int	200	600	2d14	2d14	2d12	2d12	-	-	2d10	1d14	4d14	5d12	2d14	d8@300	d8@300
	2	Ext	250	500	2d12	2d12	2d10	3d10	1d12	1d10	2d10	8d10	2d12	2d12	-	d8@300	d8@300
	2	Int	200	600	2d14	2d14	2d12	2d12	-	-	2d10	1d14	4d14	5d12	2d14	d8@300	d8@300
	3	Ext	250	500	2d12	2d12	2d10	3d10	1d12	-	2d10	5d12	2d12	3d10	-	d8@300	d8@300
	3	Int	200	600	2d12	3d12	2d10	3d10	1d12	-	2d10	2d12	6d10	6d10	2d12	d8@300	d8@300
	4	Ext	250	500	2d10	3d10	2d10	2d10	-	-	2d10	7d10	1d12	3d10	-	d8@300	d8@300
	4	Int	200	600	2d14	2d14	2d10	3d10	-	-	2d10	1d14	3d14	4d10	2d14	d8@300	d8@300
	5	Ext	250	500	2d10	3d10	2d10	2d10	-	-	2d10	5d12	1d10	2d12	-	d8@300	d8@300
	5	Int	200	600	2d16	2d16	2d12	3d12	-	-	2d10	-	2d16	1d12	1d16	d8@300	d8@300
	6	Ext	250	500	2d10	2d10	2d10	2d10	-	-	2d10	4d12	-	1d10	-	d8@300	d8@300
	6	Int	200	600	2d16	2d16	2d12	3d12	-	-	2d10	-	2d16	1d12	1d16	d8@300	d8@300
	7	Ext	250	500	2d10	2d10	2d10	2d10	-	-	2d10	1d12	-	-	-	d8@300	d8@300
	7	Int	200	600	2d16	2d16	2d12	3d12	-	-	2d10	-	1d16	-	-	d8@300	d8@300

Floor	Frame	b(mm)	h(mm)	B1.1	B1.2	B2.1	B2.2	Badd1	Badd2	Tcont	Tadd1	Tadd2	Tadd3	Tadd4	St1	St2	
K80A84	1	Ext	250	500	2d12	2d12	2d12	2d12	-	-	2d12	2d14	-	-	-	d8@300	d8@300
		Int	200	600	2d12	3d12	2d12	2d12	1d12	1d12	2d14	2d12	6d12	5d12	3d12	d8@300	d8@300
	2	Ext	250	500	2d12	3d12	2d12	3d12	1d12	-	2d14	3d12	-	-	-	d8@300	d8@300
		Int	200	600	2d14	2d14	2d12	3d12	2d12	2d12	2d14	1d14	4d14	5d12	3d14	d8@300	d8@300
	3	Ext	250	500	2d12	3d12	2d12	2d12	1d12	1d12	2d14	3d12	-	-	-	d8@300	d8@300
		Int	200	600	2d14	2d14	2d12	2d12	2d12	1d12	2d14	1d14	6d12	6d12	3d14	d8@300	d8@300
	4	Ext	250	500	2d12	3d12	2d12	2d12	1d12	-	2d14	2d16	-	-	-	d8@300	d8@300
		Int	200	600	2d14	2d14	2d12	2d12	1d14	1d12	2d14	1d14	4d14	5d12	2d14	d8@300	d8@300
	5	Ext	250	500	2d12	2d12	2d12	2d12	-	-	2d14	2d16	-	-	-	d8@300	d8@300
		Int	200	600	2d16	2d16	2d12	2d12	-	-	2d12	1d12	2d16	3d12	1d16	d8@300	d8@300
	6	Ext	250	500	2d12	2d12	2d12	2d12	-	-	2d12	3d12	-	-	-	d8@300	d8@300
		Int	200	600	2d16	2d16	2d12	2d12	-	-	2d12	1d12	2d16	2d12	1d16	d8@300	d8@300
	7	Ext	250	500	2d12	2d12	2d12	2d12	-	-	2d12	2d12	-	-	-	d8@300	d8@300
		Int	200	600	2d16	2d16	2d12	2d12	-	-	2d12	1d12	1d16	-	-	d8@300	d8@300



Floor	Frame	b(mm)	h(mm)	B1.1	B1.2	Badd1	Badd2	Badd3	Tcont1	Tcont2	Tadd1	Tadd2	Tadd3	St1	St2	
K60AEC8	1	Ext	200	500	4d12	4d12	1d16	-	-	2d14	2d12	6d12	2d16	2d16	d8@120	d8@120
		Int	200	500	4d12	4d12	2d12	-	-	2d14	2d12	6d12	3d12	3d12	d8@120	d8@120
	2	Ext	200	500	4d12	4d12	1d14	-	-	2d12	2d12	6d12	2d16	2d16	d8@120	d8@120
		Int	200	500	4d12	4d12	1d14	-	-	2d14	2d12	6d12	2d16	2d16	d8@120	d8@120
	3	Ext	200	500	4d12	4d12	-	-	-	2d12	2d12	5d12	2d12	2d16	d8@120	d8@120
		Int	200	500	4d12	4d12	-	-	-	2d12	2d12	3d12	2d12	2d12	d8@120	d8@120
	4	Ext	200	500	4d12	4d12	-	-	-	2d12	2d12	2d16	1d14	1d14	d8@120	d8@120
		Int	200	500	4d12	4d12	-	-	-	2d12	2d12	2d16	1d14	1d14	d8@120	d8@120
	5	Ext	200	500	4d12	4d12	-	-	-	2d12	2d12	1d16	-	-	d8@120	d8@120
		Int	200	500	4d12	4d12	-	-	-	2d12	2d12	1d16	-	-	d8@120	d8@120

A.2 Column schedules

Floor	Col	b(mm)	h(mm)	Reinf	Stirrups	Col	b(mm)	h(mm)	Reinf	Stirrups	Col	b(mm)	h(mm)	Reinf	Stirrups	
K60A59	1	C1	350	350	4d20	d8@300	C2	350	350	4d20	d8@250	C3	350	350	4d16+4d14	d8@250
	2	C1	350	350	4d20	d8@250	C2	300	300	4d16	d8@250	C3	300	300	8d14	d8@250
	3	C1	300	300	4d20	d8@250	C2	250	250	4d16	d8@300	C3	250	250	6d14	d8@300
	4	C1	300	300	4d20	d8@300	C2	250	250	4d14	d8@400	C3	250	250	4d14	d8@400
	5	C1	300	300	4d20	d8@400	C2	250	250	4d14	d8@400	C3	250	250	4d14	d8@400
	1	C6	350	350	4d20	d8@250	C7	350	350	4d16+4d14	d8@250	C8	350	350	4d16+4d14	d8@250
	2	C6	300	300	4d16	d8@250	C7	300	300	8d14	d8@250	C8	300	300	8d14	d8@250
	3	C6	250	250	4d16	d8@300	C7	250	250	4d18+2d14	d8@300	C8	250	250	4d18+2d14	d8@300
	4	C6	250	250	4d14	d8@400	C7	250	250	4d14	d8@400	C8	250	250	4d14	d8@400
	5	C6	250	250	4d14	d8@400	C7	250	250	4d14	d8@400	C8	250	250	4d14	d8@400

Note: All column stirrups were two-legged closed.

Floor	Col	b(mm)	h(mm)	Reinf	Stirrups	Col	b(mm)	h(mm)	Reinf	Stirrups	Col	b(mm)	h(mm)	Reinf	Stirrups	
K60A59-II	1	C1	350	350	4d20	d8@150	C2	350	350	6d16+2d18	d8@150	C3	350	350	4d18+4d14	d8@150
	2	C1	350	350	4d20	d8@200	C2	350	350	4d14+4d16	d8@200	C3	350	350	4d16+4d14	d8@200
	3	C1	300	300	4d20	d8@250	C2	300	300	4d16	d8@200	C3	300	300	8d14	d8@200
	4	C1	300	300	4d20	d8@250	C2	250	250	4d14	d8@300	C3	250	250	4d14	d8@300
	5	C1	300	300	4d20	d8@350	C2	250	250	4d14	d8@400	C3	250	250	4d14	d8@400
	1	C6	350	350	6d16+2d18	d8@150	C7	350	350	12d18	d8@150	C8	350	350	10d18	d8@150
	2	C6	350	350	4d14+4d16	d8@200	C7	350	350	4d16+4d14	d8@200	C8	350	350	4d16+4d14	d8@200
	3	C6	300	300	4d16	d8@200	C7	300	300	8d14	d8@200	C8	300	300	8d14	d8@200
	4	C6	250	250	4d14	d8@300	C7	250	250	4d14	d8@300	C8	250	250	4d14	d8@300
	5	C6	250	250	4d14	d8@400	C7	250	250	4d14	d8@400	C8	250	250	4d14	d8@400

Note: All column stirrups were two-legged closed.

	Floor	Col	b(mm)	h(mm)	Reinf	Stirrups	Col	b(mm)	h(mm)	Reinf	Stirrups	Col	b(mm)	h(mm)	Reinf	Stirrups
K70A59	1	C1	250	700	8d20	d8@400	C2	250	900	8d18+2d14	d8@150	C3	250	900	8d20	d8@150
	2	C1	250	700	8d20	d8@400	C2	250	900	8d18+2d14	d10@150	C3	250	900	8d20	d10@150
	3	C1	250	700	12d16+2d14	d8@400	C2	250	700	8d16+2d14	d10@150	C3	250	700	4d20+4d16	d10@150
	4	C1	250	700	12d16+2d14	d8@400	C2	250	700	8d16+2d14	d10@150	C3	250	700	4d20+4d16	d10@150
	5	C1	250	600	6d18+2d20	d8@400	C2	250	500	4d20+2d14	d8@150	C3	250	500	4d16+4d14	d8@150
	6	C1	250	600	6d18+2d20	d8@400	C2	250	500	4d18+2d14	d8@150	C3	250	500	4d16+4d14	d8@150
	7	C1	250	550	6d16+2d20	d8@400	C2	250	350	4d16	d8@200	C3	250	350	8d14	d8@200
	1	C6	900	250	8d18+2d14	d8@150	C7	600	600	16d20	d10@150	C8	600	600	16d20	d10@150
	2	C6	900	250	8d18+2d14	d10@150	C7	600	600	16d20	d10@150	C8	600	600	16d20	d10@150
	3	C6	700	250	8d16+2d14	d10@150	C7	500	500	4d20+8d18	d10@150	C8	500	500	4d20+8d16	d10@150
	4	C6	700	250	8d16+2d14	d10@150	C7	500	500	4d20+8d16	d10@150	C8	500	500	4d20+8d16	d10@150
	5	C6	500	250	4d20+2d14	d8@150	C7	400	400	4d16+4d18	d8@150	C8	400	400	4d16+8d14	d8@150
	6	C6	500	250	4d18+2d14	d8@150	C7	400	400	4d16+4d18	d8@150	C8	400	400	4d16+4d18	d8@200
	7	C6	350	250	4d16	d8@200	C7	300	300	8d14	d8@400	C8	300	300	8d14	d8@400

Notes: Corner columns (C1, etc) were L-shaped with 250 mm width. All column stirrups were two-legged closed.

	Floor	Col	b(mm)	h(mm)	Reinf	Stirrups	Col	b(mm)	h(mm)	Reinf	Stirrups	Col	b(mm)	h(mm)	Reinf	Stirrups
K80A84	1	C1	250	700	6d16+8d14	d8@100	C2	250	900	8d18+8d16	d8@100	C3	250	900	8d18+8d16	d8@100
	2	C1	250	700	6d16+8d14	d8@100	C2	250	900	8d18+8d16	d8@100	C3	250	900	8d18+8d16	d8@100
	3	C1	250	700	6d16+8d14	d8@100	C2	250	700	10d16+6d20	d8@100	C3	250	700	10d16+8d18	d8@100
	4	C1	250	700	6d18+7d14	d8@100	C2	250	700	10d16+6d20	d8@100	C3	250	700	10d16+8d18	d8@100
	5	C1	250	600	11d14+1d18	d8@100	C2	250	500	12d20	d8@100	C3	250	500	8d16+8d20	d8@100
	6	C1	250	600	11d14+1d18	d8@100	C2	250	500	8d18+2d14	d8@100	C3	250	500	4d20+214	d8@100
	7	C1	250	550	11d14+1d18	d8@100	C2	250	350	4d20+2d14	d8@100	C3	250	350	4d16+2d14	d8@100
	1	C6	900	250	8d18+8d16	d8@100	C7	600	600	8d20+10d18	d8@100	C8	600	600	8d20+8d18	d8@100
	2	C6	900	250	8d18+8d16	d8@100	C7	600	600	8d20+10d18	d8@100	C8	600	600	8d20+8d18	d8@100
	3	C6	700	250	10d16+4d14	d8@100	C7	500	500	14d20+6d16	d8@100	C8	500	500	8d20+12d16	d8@100
	4	C6	700	250	10d16+4d14	d8@100	C7	500	500	8d16+12d18	d8@100	C8	500	500	8d16+12d18	d8@100
	5	C6	500	250	8d20+2d14	d8@100	C7	400	400	18d20	d8@100	C8	400	400	16d20	d8@100
	6	C6	500	250	8d18+2d14	d8@100	C7	400	400	4d16+4d18	d8@100	C8	400	400	4d16+4d18	d8@100
	7	C6	350	250	4d20+2d14	d8@100	C7	300	300	8d14	d8@100	C8	300	300	8d14	d8@100

Notes: Corner columns (C1, etc) were L-shaped with 250 mm width. Perimeter column (C2, C3, C6, etc) stirrups were six-legged in the 1st and 2nd storey, five-legged in the 3rd and 4th storey, four-legged in the 5th and 6th storey and three-legged in the 7th storey, in the long direction. Interior square column (C7, C8, etc) stirrups were four-legged stirrups in the 1st to 4th storeys and three-legged in the 5th to 7th storeys.

	Floor	Col	b(mm)	h(mm)	Reinf	3-legged Stirrups	Col	b	h	Reinf	3-legged Stirrups	Col	b	h	Reinf	3-legged Stirrups
			(mm)	(mm)				(mm)	(mm)				(mm)	(mm)		
K60AEC8	1	C1	400	400	12d18+4d14	d8@100	C2	400	400	8d16+4d14	d10@100	C3	400	400	8d16+4d14	d10@100
	2	C1	400	400	8d16+4d14	d8@100	C2	400	400	8d16+4d14	d10@100	C3	400	400	8d16+4d14	d10@100
	3	C1	400	400	8d16+4d14	d8@100	C2	400	400	12d16+2d14	d8@100	C3	400	400	12d16+2d14	d8@100
	4	C1	350	350	8d20+4d14	d8@100	C2	350	350	8d20+2d16	d8@100	C3	350	350	8d20+2d16	d8@100
	5	C1	300	300	4d20+4d14	d8@100	C2	300	300	4d20+4d14	d8@100	C3	300	300	4d18+4d14	d8@100
	1	C6	400	400	8d18+4d16	d10@100	C7	400	400	8d16+4d14	d12@100	C8	400	400	12d16	d12@100
	2	C6	400	400	12d16+2d14	d10@100	C7	400	400	8d16+4d14	d10@100	C8	400	400	12d18	d10@100
	3	C6	400	400	10d16+4d18	d8@100	C7	400	400	16d16	d10@100	C8	400	400	4d20+8d16	d8@100
	4	C6	350	350	10d16+4d20	d8@100	C7	350	350	12d20	d8@100	C8	350	350	12d20	d8@100
	5	C6	300	300	4d20+4d14	d8@100	C7	300	300	4d18+4d14	d8@100	C8	300	300	4d18+4d14	d8@100

Note: All column stirrups were three-legged closed.